An Experimental Investigation of the Surface Temperature of Graphite in a Sliding System Using an Infrared Microscope

by

Melvin H. Richardson

Thesis submitted to the Graduate Faculty of the
Virginia Polytechnic Institute and State University
in partial fulfillment of the requirements for the degree of
MASTER OF SCIENCE
in
Mechanical Engineering

APPROVED:

M. J. Furey, Chairman

N. S. Eiss

H. H. Mabie

September, 1976

Blacksburg, Virginia

ACKNOWLEDGMENTS

I would like to thank Dr. M. J. Furey for having had the opportunity to work with him during the past year. His guidance and advice were invaluable.

I extend my thanks to the U.S. Army Research Office for their support of this project and to the Union Carbide Company for providing a sample of SA-35 graphite from which the test specimens were made.

I thank Dr. N. S. Eiss and Dr. H. H. Mabie for their advice.

To the typists, Mrs. Debbie Wolfe and Mrs. Libby Daws, go many thanks.

I also thank all my friends who have helped during the year and Steve Li who also worked on this project.

TABLE OF CONTENTS

LIST OF FIGURES

LIST OF TABLES

NOMENCLATURE

a	Radius of circular area of contact
c	Specific heat
E	Modulus of elasticity
f	Coefficient of friction
K	Thermal conductivity
$L = Va/2\kappa$	Peclet number
p	Load per unit area
p_m	Hardness
Q	Rate of heat supply
q	Rate of heat supply per unit area
t,T	Time
T_{mp}	Melting point temperature
V	Velocity
ε	Emissivity
$\kappa = K/\rho c$	Thermal Diffusivity
ρ	Density
σ	Poisson's ratio
θ	Temperature rise

Subscripts

B	Body B
C	Body C
m	Mean
max	Maximum

INTRODUCTION

Tribology is the name given to the discipline of study which investigates friction, wear, and lubrication. Leonardo da Vinci was one of the first to conduct investigations and report his findings (1). He reported that the force necessary to slide an object along a horizontal plane was directly proportional to the weight of the object and that this relation was true regardless of the area of contact between the two bodies. Much research has been conducted in tribology since the time of Leonardo da Vinci but some very important questions remain unanswered (22). For example, we do not know the detailed nature and distribution of the real areas of contact when one solid body slides over another. Furthermore we know very little about the actual surface temperatures produced in such systems. These two important unknowns are related.

Surface (and sub-surface) temperature are extremely important in tribology. Temperature influences the physical characteristics of the solids (e.g., hardness, elasticity) and lubricants (e.g., viscosity). And of course temperature affects the chemical behavior of the entire system (e.g., oxidation, lubricant deterioration, protective film formation). For example, Furey (21) has shown that certain metallic dithiophosphates function as antiwear additives because they are thermally unstable. In addition, his concept of "in situ" polymer film formation is based on a thermally-activated mechanism (2, 23).

The investigation conducted at Virginia Polytechnic Institute and State University has been directed toward the question of the surface

temperatures produced by bodies in sliding contact. This research was sponsored by the United States Army Research Office, with Dr. M. J. Furey as principal investigator. During the first two years of the three-year grant, an experimental apparatus was designed, built and used to obtain information on the surface temperature of polymers (3,4). Briefly this apparatus consisted of a Barnes Infrared microscope, a rotating sapphire disk against which the test specimen was loaded and various data gathering equipment (see Figure 1).

This thesis investigation is directed toward the use of graphite as the test specimen in the experimental apparatus. Graphite was chosen over other materials for several reasons. Graphite is a pure substance with well known properties. It has the potential for low wear and transfer, and high emissivity. Its practical applications include use in electrical brush contacts.

The specific goals of the present study are as follows:

[1] To adapt the experimental apparatus to measure the radiance and thereby determine the temperature in the area of contact between graphite and sapphire.

[2] To determine the temperature distribution over the area of contact.

[3] To measure the bulk temperature of the graphite test specimens.

[4] To investigate the effect on the temperature rise of sub-dividing the area of contact into a number of smaller areas of contact by using existing theories.

[5] To compare the above results with existing theories of the temperature rise in the area of contact.

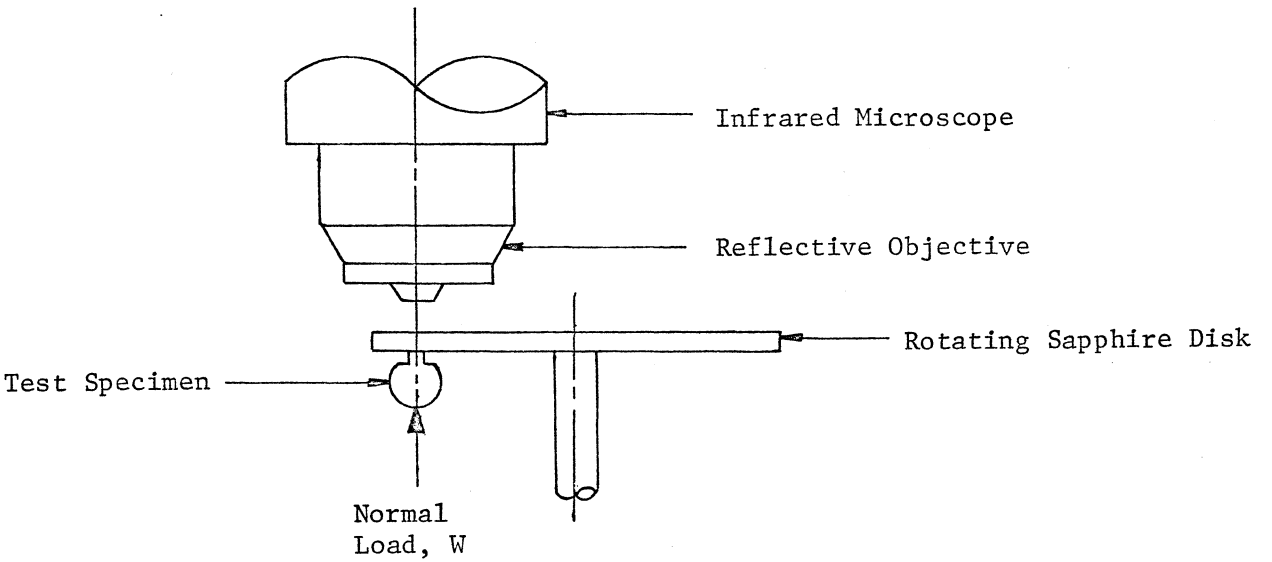

Figure 1

Basic Experimental Configuration

LITERATURE REVIEW

A. Experimental

Several experimental methods have been employed by researchers trying to measure the surface temperature in the region of contact. The three methods most often used are a) the embedded thermocouple, b) the dynamic thermocouple, and c) infrared sensors.

The embedded thermocouple has been used extensively but it has certain problems associated with it. Usually a hole is drilled in the test specimen in such a way that the thermocouple can be mounted very close to the surface of contact of the specimen. Since the thermocouple is not at the interface, it is not measuring the true interface temperature but the temperature at some finite distance away from the interface. Also the drilled hole disrupts the flow of heat in the specimen thereby complicating the analysis.

F. F. Ling and T. E. Simkins (5) used thermocouples to determine the contact surface temperature distribution of both the rider and the slider of their experimental apparatus. The experimental apparatus consisted of a rotating disk and a rider which was loaded against the circumferential face of the disk. This design is such that the flow fields of heat are two dimensional in the plane perpendicular to the interface. This allowed thermocouples to be mounted on the surface of the specimens and therefore the flow of heat was not disrupted by embedded thermocouples. The frictional resistance was recorded with different loads using one speed. The contact surface temperature distribution of the slider and the rider was determined from the data

and temperature jumps of the order of 300-700°F were observed for high Peclet numbers, L.

T. F. J. Quinn used embedded thermocouples in his study (6) of the influence of temperature on the wear of steel in an unlubricated sliding system. He found that the interface temperature can be estimated by X-ray diffraction of the wear debris. J. J. Santini and F. E. Kennedy, Jr. also used embedded thermocouples (7). In their investigation of surface temperature and wear in disk brakes, they concluded that considerable temperature gradients existed between different points on the contacting surface and that less than 25% of the nominal contact area was in actual contact at any instant. Another investigator to use embedded thermocouples was J. D. Vasilakis (8). He measured the temperature near the interface of Teflon sliding on steel in air and in a vacuum. Temperatures were recorded up to 75°C in air and 59°C in a vacuum.

The dynamic thermocouple uses the electromotive force produced by the touching of two dissimilar metals to measure the temperature. Unlike the regular thermocouple the metals are in relative motion. It will therefore give a measure of the temperature at the interface but certain limitations must be considered. The output of the dynamic thermocouple is an averaged value over the area or areas of contact and therefore discrete temperature peaks cannot be measured. The dynamic thermocouple cannot be used in a fully lubricated system since the surfaces are separated by a lubricant film. Wear and transfer of one material to the other must be considered because this could affect the electromotive force produced at the interface.

F. P. Bowden and K. E. W. Ridler (9) used the dynamic thermocouple in their investigations of the temperature rise at the interface of a sliding system. The experimental apparatus consisted of a small cylinder with one end loaded against a rotating flat annular ring. Data were also obtained on the area in contact and the friction force. The results showed that as the load or speed was increased, the surface temperature reached a maximum value. This value corresponded to the melting point of the metal.

M. J. Furey (10), and N. H. Cook and B. Bhushan (11) are others who have used the dynamic thermocouple. Furey measured the surface temperatures generated by friction in a sliding system consisting of a fixed constantan ball loaded against a rotating steel cylinder. He found that the mean surface temperature was fairly independent of running time and gross wear of the constantan ball. Also the surface temperature was affected by load and speed. Higher loads and speeds caused higher surface temperatures. Cook and Bhushan measured the temperatures between different metals using the dynamic thermocouple principle and used these temperatures to support their analysis for estimating the average interface temperature rise.

A third method of measuring interface temperatures is by the use of an infrared sensor. An infrared sensor measures the amount of radiant energy leaving a given area; from this, the temperature can be determined. A major advantage of this method is that the area under investigation is not affected. A disadvantage of this method is that one of the members of the sliding system must be transparent to infrared

radiation so that the sensor will be able to "see" the area of contact.

F. P. Bowden and P. H. Thomas (12) used a lead sulfide cell which is sensitive to infrared radiation to study the surface temperatures in a sliding system. The end of a cylindrical specimen (usually metal) was loaded against the flat surface of a rotating glass disk. The lead sulfide cell was located opposite the area of contact such that it could measure the radiant energy being emitted due to the increase in temperature. The results from this investigation also showed an increase in temperature up to the melting point of the metal.

P. Deyber and M. Godet (13) used a lead sulfide cell to measure the contact temperature in mixed friction. They found that the contact temperature follows the variation of the coefficient of friction closely. W. O. Winer (14) used a Barnes Infrared microscope to measure temperatures in sliding elastohydrodynamic point contacts. He was able to determine the temperature distribution in the oil film and on the surface of a rotating steel ball which was loaded against a sapphire plane.

Other methods have also been used to study the temperature rise at the area of contact. Bowden, Stone, and Tudor (15) used a method employing photographic plates. From earlier experiments they had determined that hot spots in the area of contact first become visible to the eye between 520 and 570°C. An apparatus was constructed which had a photographic plate on one side of a glass plane and a slider on the other. The photographic plate would then produce a trace whenever the temperature at the interface of the slider and the glass was above

520 to 570°C. Kannel and Dow (16) used vapor deposited transducers to measure the pressure and temperature in elastohydrodynamic regions.

B. Theoretical

The theoretical analysis of the temperatures in the area of contact has been made by several researchers. Most notable among these are H. Blok, J. C. Jaeger, J. F. Archard, and R. Holm.

H. Blok (17) considered several configurations of heat supply and developed a method of analysis for each. He first considered a case in which the heat was supplied to a round stationary surface. The basic assumptions made were that a) the heat was evenly distributed over the surface, b) no other heat was supplied or withdrawn such that it would affect the temperature of the round surface, and c) the temperature field would be rotationally symmetric with respect to the center of the round surface. The amount of heat, dq, applied to the small area, $rd\phi dr$, during a time interval dt, would be,

$$dq = rd\phi drqdt$$

where q is the rate at which heat is continuously supplied. The temperature rise is

$$d\theta = \frac{2\ rd\phi drqdt}{\pi\sqrt{\pi}\ \rho\ c\ 4\kappa t\sqrt{4\kappa t}}\ e^{-\frac{r^2}{4\kappa t}}$$

Performing the appropriate integration yields the temperature, θ_T, as a function of time,

$$\theta_T = \frac{1}{\sqrt{\pi}}\ \frac{qa}{K}\left\{\frac{1}{\sqrt{X}}\left(1-e^{-X}\right) + 2\int_{\sqrt{X}}^{\infty} e^{-x^2}dx\right\}$$

where $X = \frac{a^2}{4\kappa T}$. This configuration was also analyzed for a heat source of parabolic distribution. In addition, Blok considered a square

surface with the heat supply evenly distributed and parabolic.

Next, the case of two bodies pressed together with surface 1 having a circular protuberance in contact with the plane surface of body 2 was considered. The heat supply was assumed evenly distributed over the interface and also the assumption was made that no temperature jump existed across the interface between a point on body 1 and a contacting point on body 2. Blok then considered the case of relative motion of the two bodies. The velocity is important in this case. At higher velocities the side flow of heat will be reduced and the maximum temperature rise will occur to the rear of the center of contact.

The case in which the heat is generated by friction between the two bodies in relative motion is of great interest in tribology. If the velocity is low ($V \leq \left[\frac{1}{25}\right] 4 \kappa_2/a$) the moving body 2 may be treated as a stationary body. The temperature rise at the center of contact may be approximated by,

$$\theta \approx \frac{qa}{K_1 + K_2} \tag{1}$$

If the velocity is high ($V \geq [5] 4 \kappa_2/a$) body 2 tends to absorb more of the heat. The problem arises in that the heat is not evenly distributed over the contact area and it is not distributed in the same manner over both bodies. Blok used the average value between the two temperature distributions since the assumption was made that no temperature jump existed. The maximum temperature rise is then,

$$\theta_{max} = \frac{2fp}{\rho_2 c_2} \frac{(1 + 1/\sqrt{2})\ \phi_2}{\kappa_1/\kappa_2 + \frac{\pi}{2}\phi_2} \qquad (2)$$

where $\phi_2 = Va/4\kappa_2$.

J. C. Jaeger (20) presented a comprehensive analysis of the temperature rise involving moving sources of heat. He chose a band source and a rectangular source as the shapes of the surface of contact. Numerical results are given for the specialized case of the square source and comments are made concerning a circular source. The basic assumptions made in his analysis are a) uniform plane source of heat, b) source of heat moves with a constant velocity in the surface of a semi-infinite medium, and c) no heat loss from the surface.

Jaeger introduced the Peclet number, L,

$$L = Va/2\kappa$$

as a dimensionless parameter to be used in accounting for the effect of velocity on the temperature rise. He developed analytical expressions for the temperature rise for low values of L ($L < 0.1$) and for high values of L ($L > 5.0$); however, curves must be used for the temperature calculation for intermediate values of L ($0.1 < L < 5.0$).

Jaeger obtained solutions for moving heat sources by integration of the fundamental equations of the temperature at a point and along a line in an infinite solid. His solutions included the steady temperature due to a band source and a rectangular source moving with a constant velocity. The stationary source and the case in which motion of the source had taken place for a finite time were also presented.

Jaeger considered two configurations when applying these results to a sliding system. One was that of a protuberance on a semi-infinite body sliding on the smooth surface of another semi-infinite body; the other was a long thin slider (e.g., a rod) sliding along a semi-finite body. For the case of the long thin slider, the heat loss due to radiation from its sides was taken into account. He made the assumption that the division of heat between the two bodies, for all configurations, would be based on the condition that the average temperature should be the same on the surface of each of the two bodies at the interface.

For the case of a square protuberance of one body sliding on the smooth surface of another body the average temperature, θ, over the area of contact is,

$$\theta = 0.946 \frac{q\ell}{K_1 + K_2} \qquad \text{for} \quad L < 0.1 \tag{3}$$

$$\theta = \frac{1.064\ q\ell\kappa_1^{1/2}}{1.125\ K_2\kappa_1^{1/2} + K_1\ (\ell V)^{1/2}} \qquad \text{for } L > 5.0 \tag{4}$$

For intermediate values of L, a curve must be used to determine the temperature.

The average temperature, θ, in the second case, that of a square rod sliding on a smooth semi-infinite body, is given by,

$$\theta = \frac{0.946\ q\ell}{K_1 + 1.338\ (\ell K_2\varepsilon)^{1/2}} \qquad \text{for} \quad L < 0.1 \tag{5}$$

$$\theta = \frac{1.064\ q\ (\kappa_1 \ell)^{1/2}}{K_1 V^{1/2} + 1.504\ (\kappa_1 K_2 \varepsilon)^{1/2}} \quad \text{for } L > 5.0 \tag{6}$$

Again for intermediate values of L a curve must be used to determine the temperature.

J. F. Archard (18) recognized the need for a theory which emphasized the physical considerations and reduced the mathematical complexities. His analysis was based on the assumptions that a) the heat is generated at the true area of contact (single continuous circular area) and b) the heat is conducted away into the bulk of the rubbing members. In his model, a protuberance on body B moves across body C; therefore body B receives heat from a stationary heat source and body C receives heat from a moving heat source. He also used the Peclet number as a dimensionless parameter to be used in accounting for the effect of the velocity on the temperature rise.

Body B always receives heat from a stationary source and the temperature rise, θ_B, equals

$$\theta_B = \frac{Q_B}{4aK_B} \tag{7}$$

For low velocities ($L < 0.1$), body C may also be treated as receiving heat from a stationary source and the temperature rise, θ_C, equals

$$\theta_C = \frac{Q_C}{4aK_C} \tag{8}$$

For high velocities ($L > 5.0$), the flow of heat in body C can be treated as one-dimensional because of the small amount of time of contact. The temperature on the surface of a semi-infinite solid

which receives heat at a constant rate is given by Archard as

$$\theta = \frac{2\, qt^{1/2}}{(\pi\, K\rho c)^{1/2}}$$

To apply this equation to body C (a fast moving contact) let

$$q = \frac{Q_C}{\pi a^2}$$

and consider the effective value of time for any point within the contact. The average temperature, θ_m, is then obtained as,

$$\theta_m = \frac{0.31\, Q_C}{K_C\, a} \left(\frac{\kappa_C}{Va}\right)^{1/2} \tag{9}$$

For moderately low speeds ($0.1 < L < 5.0$) a factor, α, which is a function of L must be introduced into the equation for a stationary source (18). This factor ranges from about 0.85 at L = 0.1 to about 0.35 at L = 5.0.

To take into account the division of heat between the two bodies, Archard proposed the following method for calculating the mean temperature rise. First calculate the temperature rise of body B assuming all the heat is supplied to it. Then calculate the temperature rise of body C assuming all the heat is supplied to it. The mean temperature rise of the system, θ_m, will then be given by

$$1/\theta_m = 1/\theta_B + 1/\theta_C \tag{10}$$

R. Holm (18) also was interested in reducing the mathematical complexities of surface temperature calculations. His approach was

that of approximating the actual flat, circular contacting spot and curved lines of heat flow by a sphere of infinite conductivity, zero heat capacity and straight, radial lines of heat flow. The radius of the sphere, b, is given by,

$$\pi b = 2a$$

where a is the radius of the circular contact spot. This equation was based on the principle that the same amount of generated heat should cause the same average temperature rise in the actual and the substituted contact. To simplify the calculations a dimensionless parameter, Z, was introduced which lumps together both the time and space variables. A graph was presented which shows Z vs. a function of Z, B(Z), that is used in the simplified calculations.

In his analysis of a circular heat source moving on the surface of a semi-infinite body, Holm assumes the frictional heat is produced at a uniform rate over the entire contact area. The dimensionless parameter Z was defined as

$$Z = \frac{\pi^2}{4} \frac{K}{ca^2} t$$

But the average contact time with a moving circular heat source is

$$\bar{t}_v = \frac{\pi}{2} \frac{a}{V}$$

Substituting this into the equation for Z gives

$$Z_v = \frac{\pi^3}{8} \frac{K}{caV}$$

This value is used to determine $B(Z_V)$ from the graph which is used in the equation for the maximum temperature rise, $\vartheta_m(V)$, above the ambient temperature where

$$\vartheta_m(V) \approx B(Z_V)\,\theta_m = B(Z_V)\,\frac{aq}{K} \tag{11}$$

The differences in the theories are a result of the simplifying assumptions that were made during their development. The theories of Blok and Holm predict the maximum temperature rise while those of Archard and Jaeger predict the mean temperature rise. All the theories assume that no temperature discontinuity exists across the interface but different methods were used to apply this constraint. The effect of velocity was taken into account in all the theories. Archard, Jaeger, and Blok presented different equations for the different speed regimes (i.e., low, intermediate, and high speed) but Holm used one basic equation along with a multiplication factor to account for velocity. The difference in the low speed equations of Archard and Jaeger is due solely to the fact that Archard assumed a circular area of contact and Jaeger assumed a square area of contact. The high speed equations differ because Archard and Jaeger used a different method to apply the constraint that no temperature discontinuity existed across the interface. Effects of load and friction are included in each equation by the term containing the rate of heat supplied to the contact area.

EXPERIMENTAL

A. Description of Apparatus

The experimental apparatus was designed to measure the friction force and the radiance at the interface of a sliding system (see Figure 2). The sliding system consists of a specimen loaded against a rotating sapphire disk (see Figure 3). By measuring the radiance from the area of contact, the temperature at the area of contact could be calculated. The friction force data was used in the theoretical calculation of surface temperature.

A Barnes Infrared Microscope (Model RM-2A) was used to measure the radiance at the interface of the sliding system. The microscope consists of a microscope unit and a control unit. The microscope unit has a reflecting objective lens for collecting target energy, a visible light channel for viewing the target and an infrared optical channel. The infrared energy is sensed by an indium antimonide detector which produces an electrical signal directly proportional to the infrared radiation level. A 36X reflecting objective with a resolution of 1.778×10^{-5}m was used in this investigation. The visible light channel has a 10X eyepiece for a total magnification of 360X. The control unit contains the electronic processing circuits and controls for operating the microscope. A complete description of the Barnes Infrared Microscope may be found in reference 20. A Barnes Model RM121-1 Calibration Source was used to calibrate the microscope (see Appendix A).

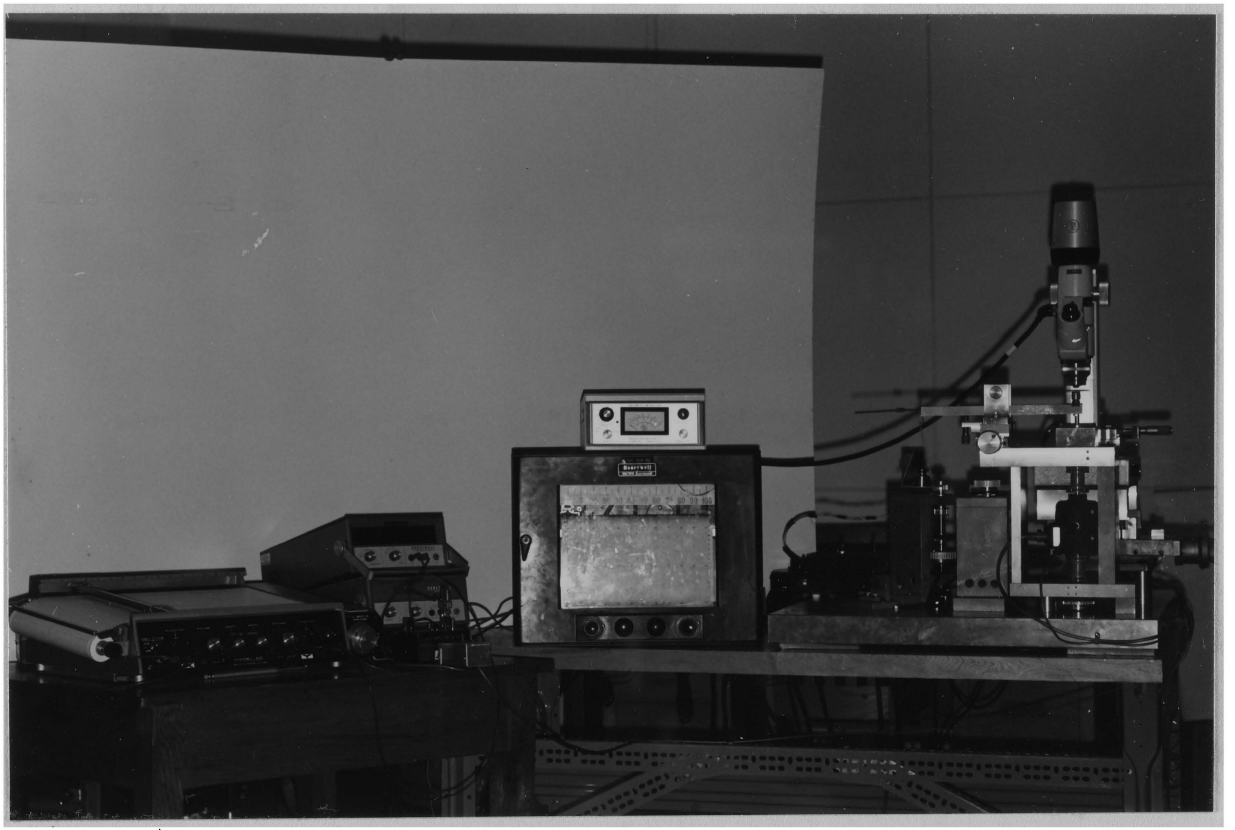

Figure 2. Overall View of Experimental Apparatus

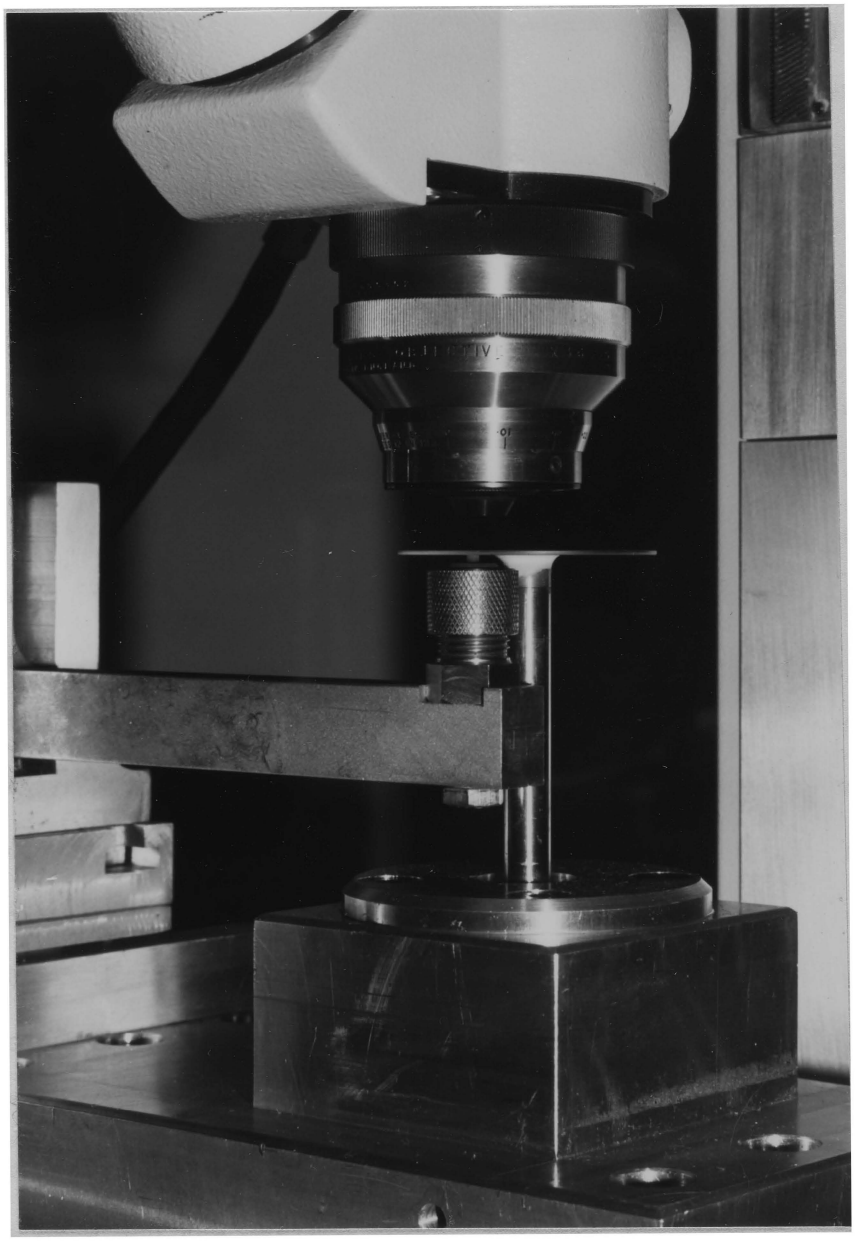

Figure 3. The Test Specimen Loaded Against the Sapphire Disk.

The microscope was mounted on a precision X-Y table (see Figure 4). Linear variable differential transformers (LVDT's) were also mounted to the table in the X and Y directions. Thus the position of the microscope could be accurately determined. The output from an LVDT was used to drive one channel of an X-Y recorder so that a plot of radiance vs. position was obtained. It was necessary to use an Omega DC Amplifier to match the input impedance of the X-Y recorder to the output of the LVDT. Without the DC amplifier the X-Y recorder would alter the output of the LVDT.

The output from the microscope was fed into one channel of a Moseley Model 2D X-Y Recorder. An Omega DC Amplifier was required in the circuit between the microscope and the X-Y recorder so that the output of the microscope would not be altered by the recorder. The other channel of the X-Y recorder could be set to a time base or to receive the output from an LVDT. Therefore a plot of radiance vs. time or a plot of radiance vs. position could be obtained. A Honeywell 620B Digital Voltmeter was used to monitor the output from the microscope.

The specimen was loaded against the sapphire disk by means of a balance beam (see Figure 5). The specimen was held at one end of the beam and the desired normal load was obtained by adding weights to a bowpan (after counterbalancing) which was hung from the other end. Since the beam was pivoted in the center, the applied normal load was equal to the amount of force (weight) in the bowpan. This entire assembly was mounted on a linear displacement slide so the specimen

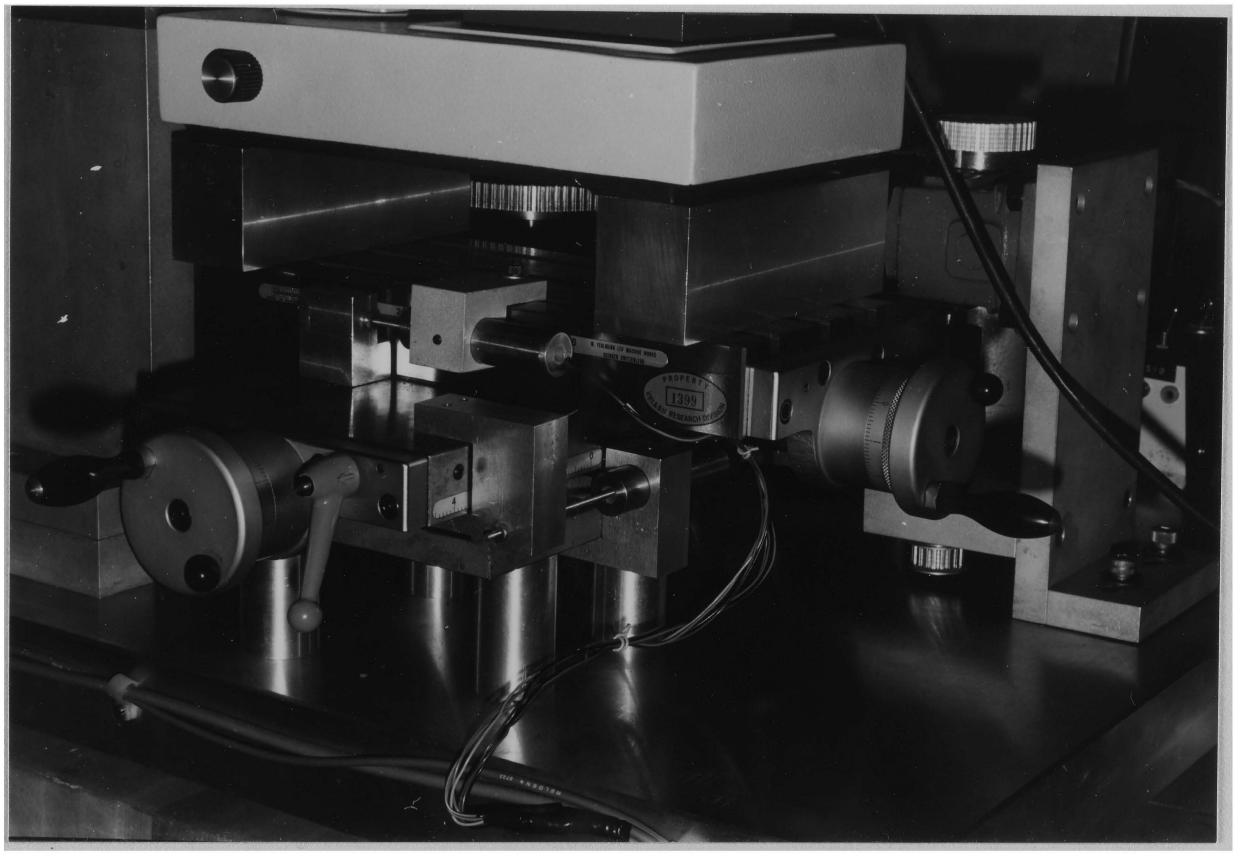

Figure 4. The Precision X-Y Table and the LVDT's.

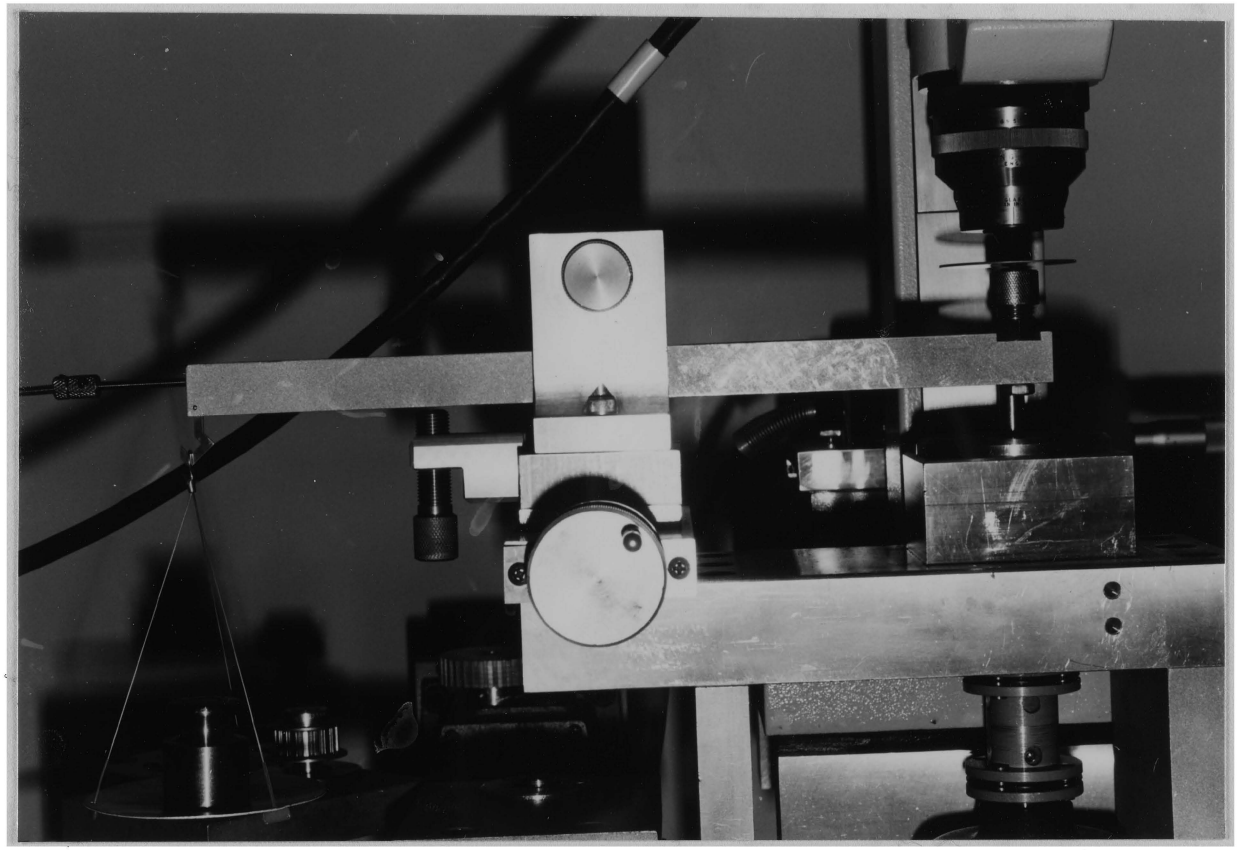

Figure 5. The Balance Beam.

could be positioned at any desired radial distance on the sapphire disk.

The disk was driven through a series of pulleys and belts by a hysteresis synchronous motor (see Figure 6). This arrangement allowed a large variation in the selection of speeds (from 1.125 rpm to 7200 rpm).

A Lebow miniature rotary torque transducer was used in the measurement of the friction force (see Figure 7). The input shaft was driven by the belt and pulley arrangement and the sapphire disk was mounted on the output shaft. The output of the torque transducer was recorded by a Honeywell Brown Electronik chart recorder. The friction force and the coefficient of friction could then be determined from these data.

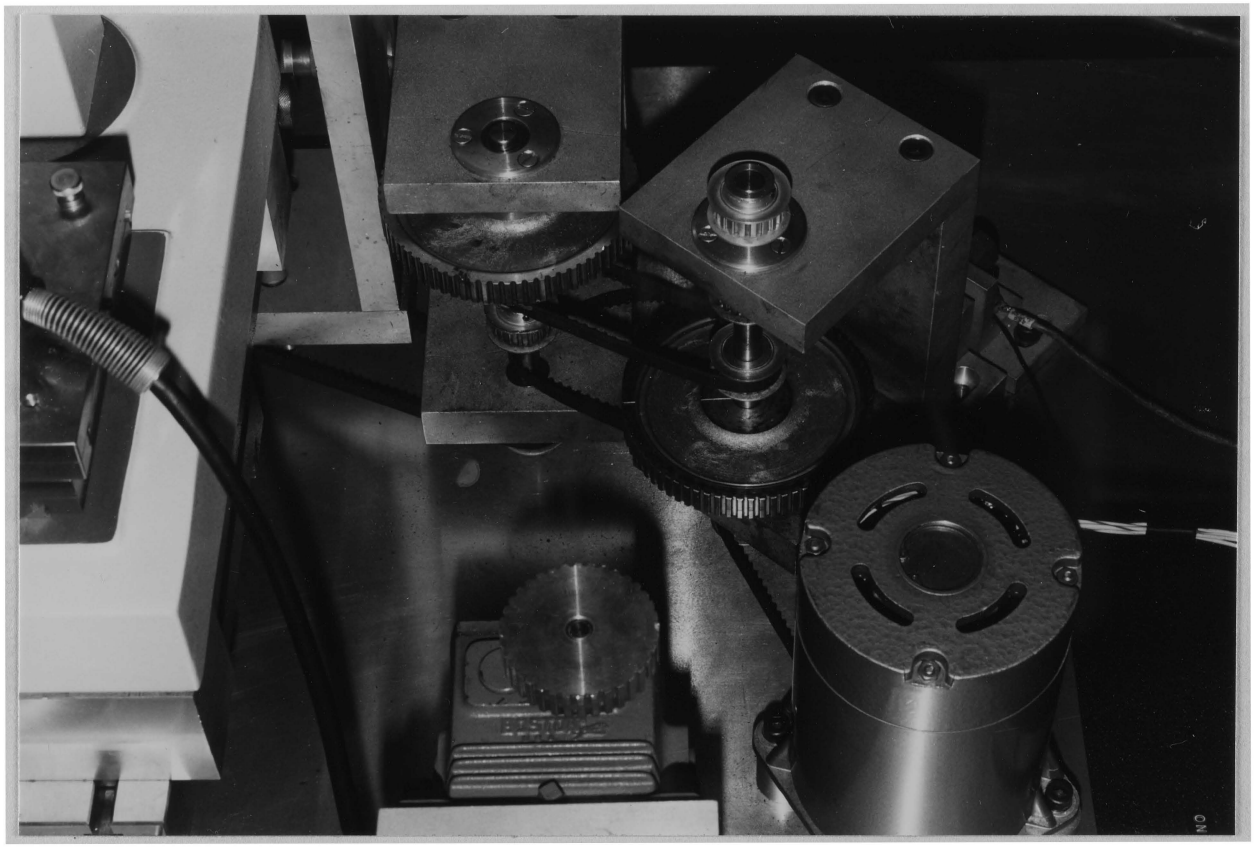

Figure 6. The Drive System for Rotating the Sapphire Disk.

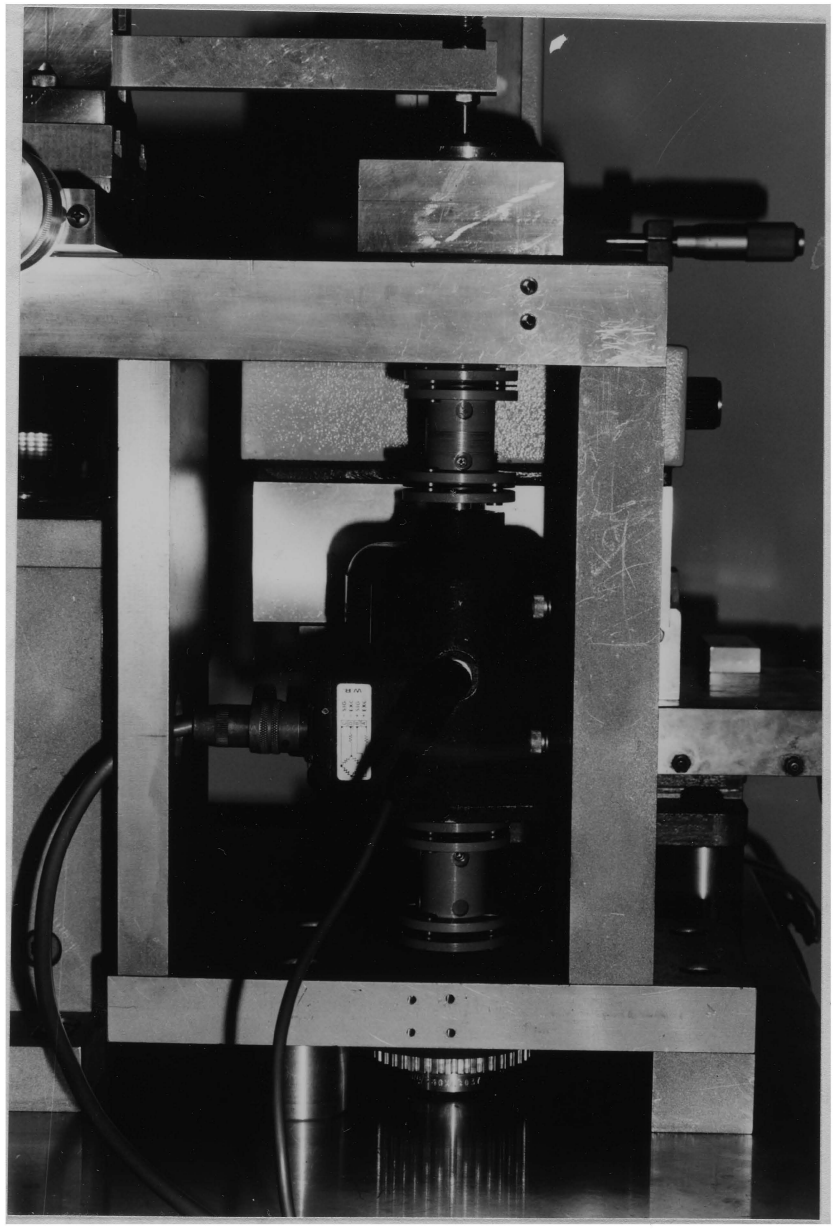

Figure 7. The Torque Transducer

B. Test Procedure

Before beginning a test, the sapphire disk and graphite specimen were cleaned. The sapphire was cleaned with several different chemicals (tri-sodium phosphate, nitric acid, hexane, and acetone) and rinsed with distilled water between each cleaning. The graphite specimen was cleaned by heating it to a dull red glow and immersing it in distilled water. It was then dried in a vacuum oven. Appendices B and C give the details of the cleaning procedures.

The instrumentation was turned on and given a warm-up period (about one-half an hour) in which to stabilize. The specimen was mounted in its holder, loaded against the sapphire disk and the microscope focused on the center of the area of contact. The specimen was then taken out of contact with the disk and the motor turned on. The output of the torque transducer (i.e., the torque due to the frictional resistance of the bearings) was set to zero on the Honeywell recorder. Thus the Honeywell recorder was recording only the friction force generated at the interface of the specimen and the sapphire disk. The motor was then stopped and the specimen loaded against the disk with the appropriate normal load. The LVDT's were adjusted to the null position.

Next the microscope was zeroed by blocking the objective with a rough surface (e.g., a paper towel) at room temperature. The Moseley X-Y Recorder was turned on with the X axis selector set to the time function and the Y axis selector set to an appropriate scale factor for the expected radiance output. The rough surface was removed from the

objective and the motor started. The output of the microscope could then be observed on the digital voltmeter or on the plot on the Moseley X-Y recorder and the output of the torque transducer could be observed on the Honeywell recorder.

If the test was to include a scan of the contact area, the following procedure was used. The output of the microscope was allowed to reach equilibrium. The LVDT selector switch was set to either the radial or the tangential position depending on the desired direction of the scan. The X axis selector on the Moseley recorder was set to millivolts so it could respond to the output of the LVDT that was selected. The microscope was then moved across the area of contact in the selected direction by use of the X-Y table. Therefore the Moseley recorder generated a plot of radiance vs. position along a line in the contact area. The microscope was then indexed the desired distance in the direction perpendicular to the previous scan and another scan was made. Using this procedure the entire area of contact could be scanned. Thus the temperature distribution over the area of contact could be determined.

C. Test Specimens

Amorphous graphite was chosen as the material for the test specimens. It is a pure substance with well known properties, the potential for low transfer and wear, and high emissivity. The Union Carbide company supplied a sample of SA-35 graphite which is used as the basic brush material for sliding electric contacts. This graphite is made by mixing lampblack with a petroleum binder and subjecting it to high temperature and pressure. The average value of the properties of SA-35 graphite (at room temperature) were also supplied by Union Carbide (see Table 1).

Although test specimens in previous investigations were spherical, a different geometry was chosen for this study (Figure 8). The upper section of a 1.77×10^{-2}m diameter spherical specimen was machined in such a manner that a cylindrical protrusion with a flat end remained. Three different diameters of the cylindrical protrusion were chosen and two specimens of each diameter were made. With these six test specimens, two important parameters affecting the temperature rise in the area of contact could be studied; namely a) the apparent area of contact and b) velocity. Table 2 gives the dimensions of the test specimens and the experimental conditions. Four of the specimens had a small hole (5.08×10^{-4}m in diameter) drilled radially from the spherical surface to the center of the specimen. A thermocouple was inserted in this hole so the bulk temperature of the graphite could be measured throughout a test. With this geometry, the same holder could be used and the flat end of the cylindrical protrusion could be seated

Table 1

Physical Properties of Graphite and Sapphire

	Graphite[a]	Sapphire[b]
Modulus of Elasticity, E (N/m^2)	5.52×10^9	3.65×10^{11}
Density, ρ (Kg/m^3)	1.55×10^3	3.98×10^3
Specific Heat, c ($J/Kg-^oC$)	7.12×10^2	4.20×10^2
Thermal Conductivity, K ($J/s-m-^oC$)	2.90×10^1	4.18×10^2
Thermal Diffusivity, $\kappa = K/\rho c$ (m^2/s)	2.63×10^{-5}	2.50×10^{-5}
Hardness, P_m (N/m^2)	2.55×10^8	1.77×10^{10}
Melting point, T_{mp} (^oC)	3.50×10^3	2.31×10^3
Poisson's Ratio, σ	1.20×10^{-1}	2.00×10^{-1}

[a]Source: Union Carbide Corporation, Carbon Products Division, Parma, Ohio

[b]Source: General Ruby and Sapphire Corporation, New York, New York

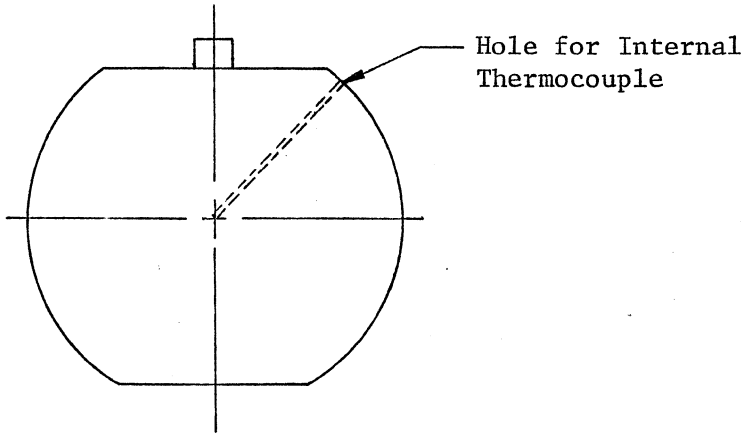

Figure 8

Test Specimen Geometry

Table 2

Test Conditions

Test Specimen	Diameter of Protrusion (m)	Height of Protrusion (m)	Normal Load (N)	Sliding Velocity (m/s)
G-1-P	2.54×10^{-3}	1.02×10^{-3}	1.96	0.817
G-2-P	1.27×10^{-3}	1.02×10^{-3}	1.96	0.817
G-3-P	6.35×10^{-4}	1.02×10^{-3}	1.96	0.817
G-4-P	2.54×10^{-3}	1.02×10^{-3}	1.96	3.267
G-5-P	1.27×10^{-3}	1.02×10^{-3}	1.96	3.267
G-6-P	6.35×10^{-4}	1.02×10^{-3}	1.96	3.267

against the sapphire disk easily.

The scanning electron microscope was used to take photographs of the test specimens before (Figure 9 and 10) and after the tests (see Results section). The actual areas of contact could be approximated from these photographs.

The sapphire disk was obtained from General Ruby and Sapphire Corporation, New York. It was 5.08×10^{-2} m in diameter and 1.02×10^{-3} m thick. The properties of the sapphire (at room temperature(are given in Table 1.

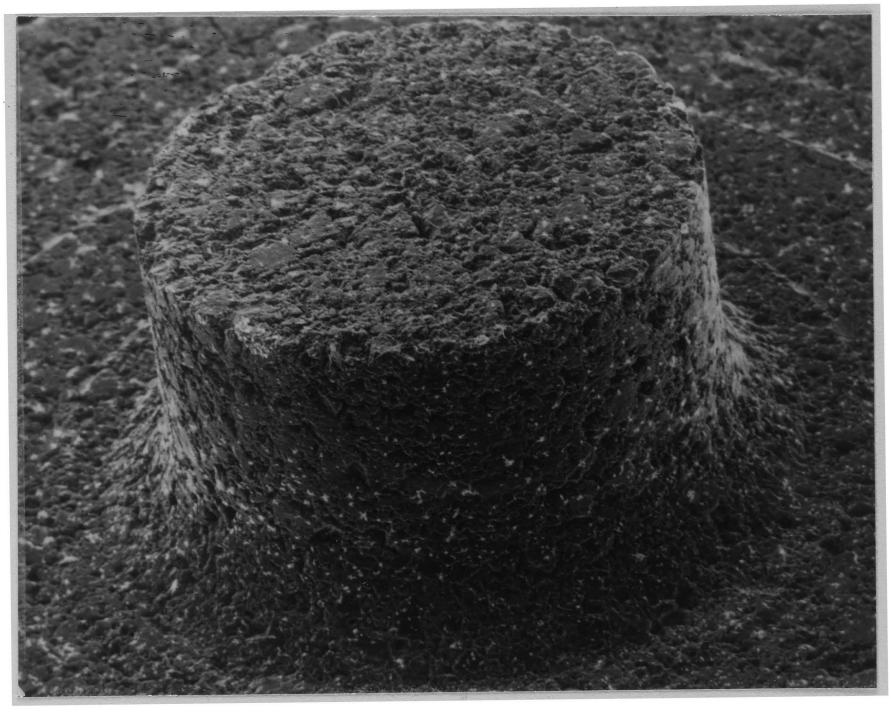

(40X)

Figure 9

Scanning Electron Microscope Photograph of a Typical Proturberance on a Graphite Test Specimen Before Testing

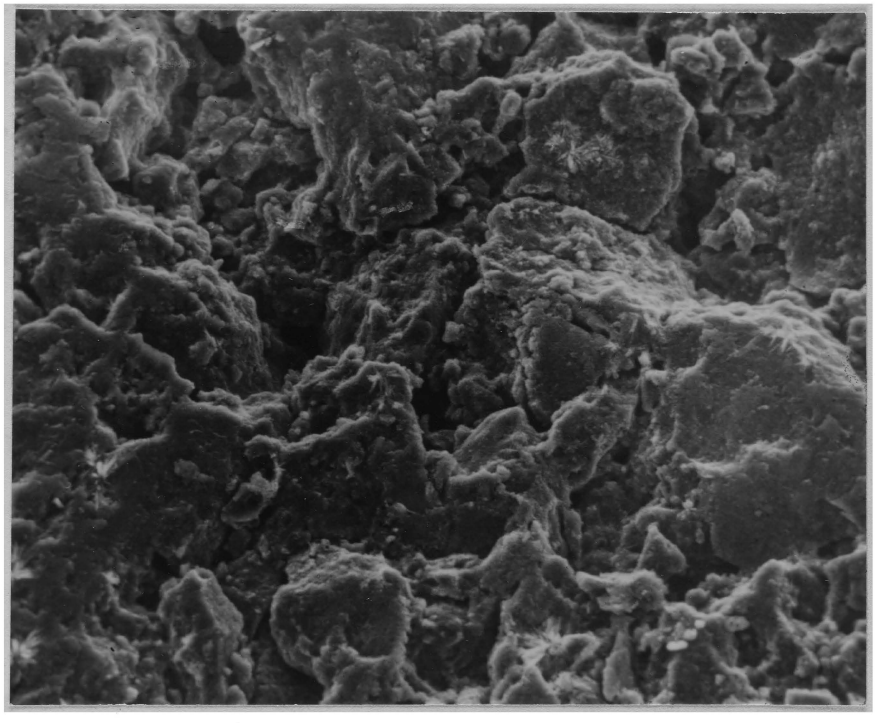

(400X)

Figure 10

High Magnification Photograph of the Surface of SA-35 Graphite Before Testing

D. Emissivity of the Graphite Test Specimens

Since the value of the emissivity of the specimen was used in the calculation of the surface temperature, it was necessary to measure it accurately. Certain questions must be considered in making this measurement. Is the emissivity of the graphite the same when in contact with the disk and when not in contact? Is the emissivity of a wear spot on the graphite the same as that of the machined surface? The following procedure was used to answer these questions and to determine the value of the emissivity to be used.

A 6.35×10^{-3} m diameter graphite sphere was made with a small radial hole drilled in it. The hole was ten times its diameter in depth and would therefore approximate a black body cavity. Another small hole was drilled near the first so a thermocouple could be inserted to measure the temperature. This specimen was placed in the holder on the balance beam which had been modified so it could be heated with a soldering iron. The temperature of the soldering iron was controlled by a Variac. A wear spot was made on the specimen near the black body cavity. Several different measurements were made using the following procedure.

The Variac was adjusted to a setting and the temperature of the specimen was allowed to stabilize. Readings were then taken with the microscope focused on the surface, on the wear spot, and on the black body cavity. The specimen was then moved underneath the sapphire disk and loaded against it with a 4.903 N load. The temperature was allowed to stabilize and readings were again taken of the surface,

the wear spot and the black body cavity each in contact with the disk. This procedure was repeated for different settings on the Variac.

RESULTS

A. Experimental

All the tests were conducted in a room with controlled temperature and humidity. The temperature was maintained at 20°C (±1°C) and the relative humidity was 51% (±1%). The actual time of each test varied depending on the number of scans made. The test durations ranged from 50 minutes to 1 hour, 28 minutes except that for one specimen which broke after 3.6 minutes.

The results of the emissivity measurements of graphite are shown in Tables 3 and 4. The values obtained from a wear spot on the graphite are lower than those obtained from the "as machined" surface. Figure 11 shows the emissivity values of a wear spot as a function of temperature.

A typical trace of radiance as a function of time is shown in Figure 12. At the start of a test the radiance would increase quickly and then climb to equilibrium. Equilibrium was reached in about five minutes in all tests except for G-6-P in which the specimen broke after 3.6 minutes. Figure 13 shows a typical trace of radiance as a function of position across the top of the protuberance. The edges of the protuberance are easily determined. In tests G-2-P and G-4-P a high-pitched noise, originating at the area of contact, was noticed. It occurred randomly and had no observable effect on the temperature or the friction force. No wear debris was evident in any of the tests. Transfer of graphite to the sapphire disk was minimal.

Table 3

Emissivity Values of the Surface of the Graphite Specimens

Variac Setting	Position of Specimen*	Thermocouple Temperature (°C)	Microscope Output (mv)		Emissivity
			Surface	Black Body Cavity	
30.0	A	25.5	6	10	0.60
	B	25.5	23	26	0.88
50.0	A	32.0	18	42	0.42
	B	37.5	74	84	0.88
70.0	A	43.0	35	85	0.41
	B	46.0	135	152	0.88
90.0	A	53.0	85	169	0.50
	B	60.3	250	287	0.87

Average emissivity A - 0.48

B - 0.88

---

* A - Data taken with specimen in contact with sapphire disk.

B - Data taken directly from surface of specimen.

Table 4

Emissivity Values of a Wear Spot on the Graphite Specimens

Variac Setting	Position of Specimen*	Thermocouple Temperature (^{o}C)	Microscope Output (mv)		Emissivity
			Wear Spot	Black Body Cavity	
30.0	A	25.5	5	15	0.33
	B	26.0	9	20	0.45
50.0	A	28.6	13	34	0.38
	B	32.0	31	59	0.52
70.0	A	37.8	36	78	0.46
	B	45.0	76	127	0.59
90.0	A	48.3	76	130	0.58
	B	55.0	149	235	0.63

Average emissivity A - 0.44

B - 0.55

* A - Data taken with specimen in contact with the sapphire disk.

B - Data taken directly from surface of specimen.

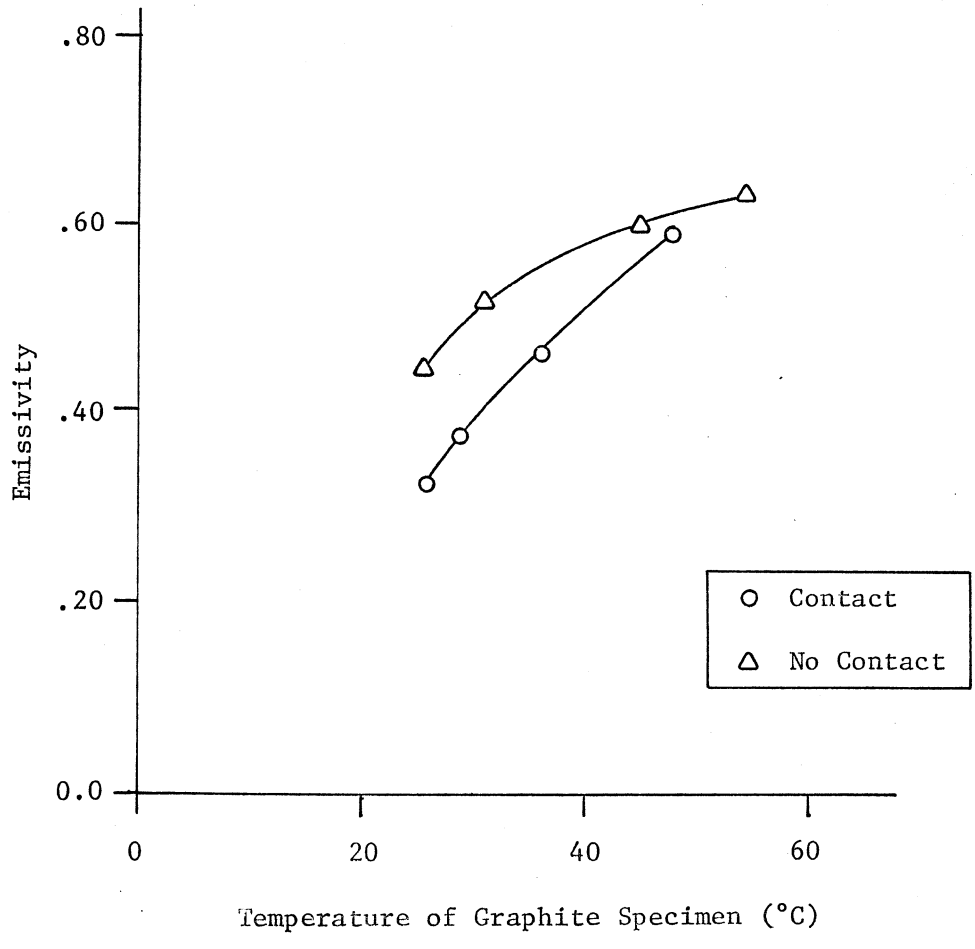

Figure 11

Emissivity Values of a Wear Spot as a Function of Temperature

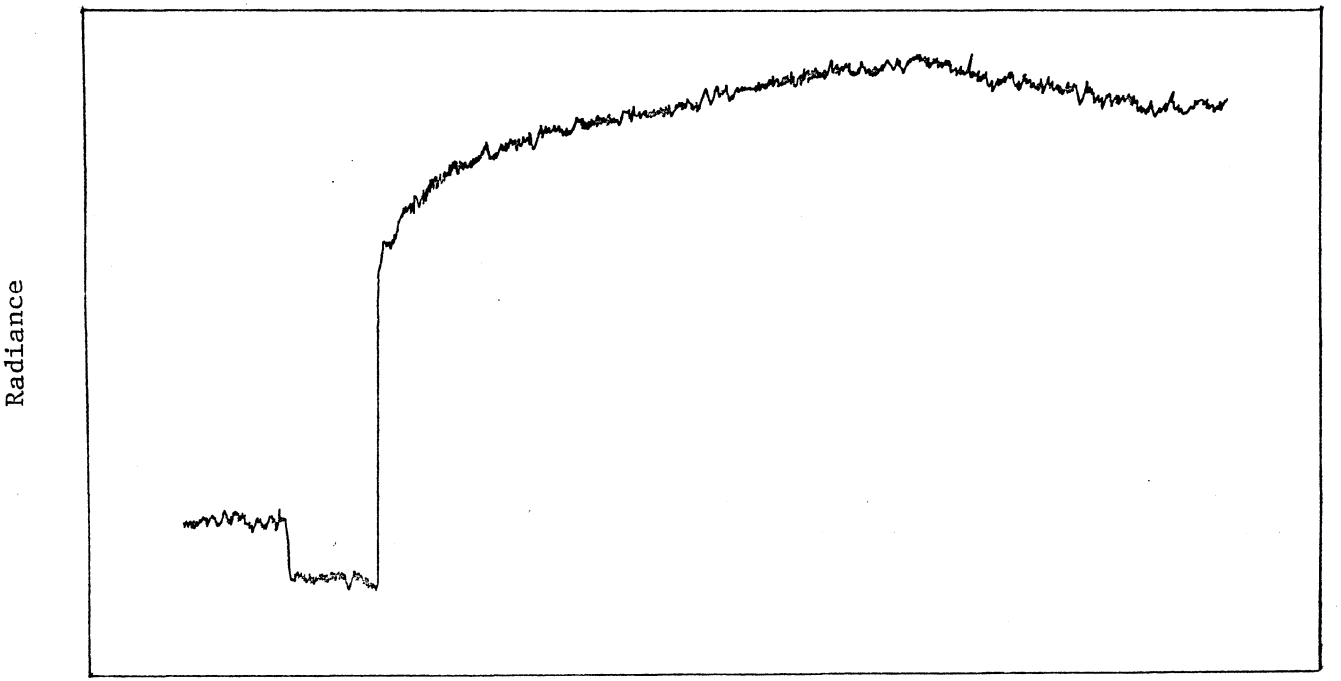

Figure 12

Typical Plot of Radiance as a Function of Time

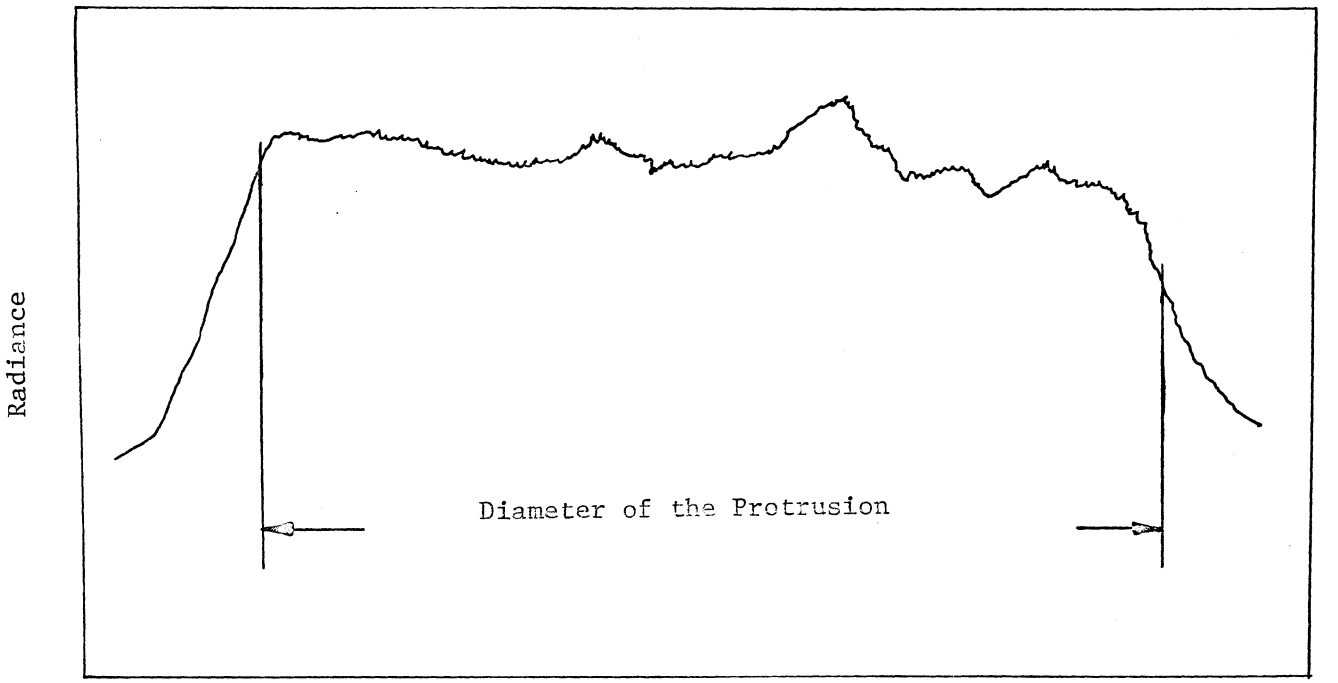

Figure 13

Typical Plot of Radiance as a Function of Position

To determine the temperature rise from the radiance data the procedure given in Appendix H must be used. However the proper emissivity value to be used in these calculations must be determined. Two approaches may be used since emissivity is a function of temperature. One approach would be to use an iteration procedure in which the temperature rise is calculated based on an assumed emissivity. This calculated temperature could then be used to select a new value for the emissivity. After several iterations a final emissivity value would be obtained which corresponded to the approximate temperature rise. Table 5 shows the results of calculations based on this procedure. Since some of the calculated temperature rises are beyond the range of the data obtained for emissivity as a function of temperature, the emissivity closest to the approximate temperature rise was used for these cases.

Another approach would be to use an average emissivity value. Table 6 gives the mean temperature rise at equilibrium using each of the four average values shown in Tables 3 and 4. The average emissivity value for a wear spot in contact with the sapphire disk (i.e.,0.441) is used for all other temperature calculations presented in this thesis.

Table 7 gives the temperature rise above ambient at the center of contact and the maximum temperature rise in the area of contact. Also shown is the bulk temperature rise of the graphite as measured by an embedded thermocouple. (No data were obtained for G-1-P or G-4-P.) The bulk temperature rise of each specimen was insignificant except for G-5-P where it was approximately 10% of the mean temperature rise.

Table 5

Experimental Temperature Rise Based on Emissivity as a Function of Temperature

Specimen	Emissivity Used in Mean Temperature Calculation	Mean Temperature Rise (^{o}K)	Emissivity Used in Maximum Temperature Calculation	Maximum Temperature Rise (^{o}K)
G-1-P	0.33	6.5	-	-
G-2-P	0.42	12.5	0.56	22.0
G-3-P	0.43	13.5	0.46	18.5
G-4-P	0.54	20.5	0.58	30.0
G-5-P	0.58	36.1	0.58	40.6
G-6-P*	0.58	36.5	-	-

* Data after 3.6 minutes, not at equilibrium

Table 6

Experimental Mean Temperature Rise Based on Average Emissivity

Specimen	Mean Temperature Rise (^{o}K)			
	ε = .44	ε = .48	ε = .55	ε = .88
G-1-P	5.5	4.4	4.3	3.5
G-2-P	12.4	11.0	10.0	6.0
G-3-P	13.4	12.5	11.0	7.5
G-4-P	24.0	22.0	20.0	14.5
G-5-P	43.6	40.6	37.6	27.1
G-6-P*	43.5	40.0	36.5	27.0

*Data after 3.6 minutes, not at equilibrium.

Table 7

Experimental Results at Equilibrium

Specimen	Radiance of Center of Contact Area (W/cm^2-ster) x 10^{-3}	Temperature Rise at Center of Contact (^oK)	Maximum Temperature Rise in Contact Area (^oK)	Bulk Temperature Rise of Specimen (^oK)
G-1-P	0.594	5.5	-	-
G-2-P	1.544	12.4	25.5	0.0
G-3-P	1.743	13.4	18.5	0.3
G-4-P	3.645	24.0	35.5	-
G-5-P	8.715	43.6	48.5	4.5
G-6-P*	8.794	43.5	-	0.5

* Data after 3.6 minutes, not at equilibrium.

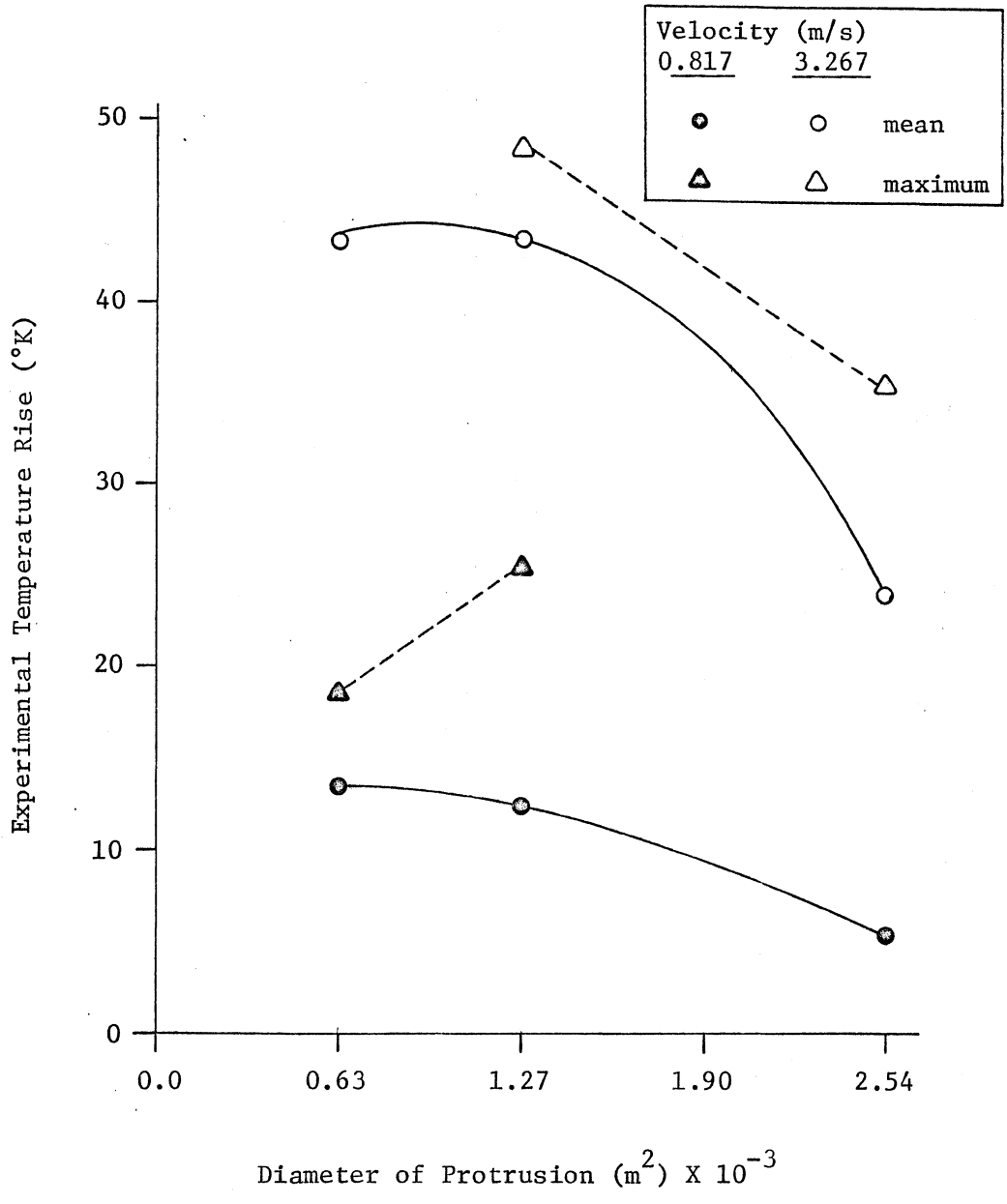

Figure 14

Diameter of Protrusion vs. Experimental Temperature Rise

The temperature rise distributions above ambient for each specimen are shown in Figures 15 to 18. No temperature rise distribution is shown for G-1-P because of insufficient data or for G-6-P since it broke after 3.6 minutes. The actual areas of specimen G-3-P that were in contact with the sapphire disk are shown by the dashed lines. This information is not shown on the other temperature rise distributions because of the complicated nature of the actual areas of contact. However, the relationship between the actual areas of contact and the temperature rise above ambient can be seen by referring to the scanning electron micrographs shown in Figures 19 to 24. Figure 25 is a close-up of an area which was in contact with the disk.

These micrographs were used to approximate the true areas of contact (darker areas) for each specimen. An estimate of the true area of contact was made in two ways. A photographic enlarger was used to project the scanning electron microscope negatives onto a large piece of paper and the areas of contact were traced with a pencil. These areas were then cut out and weighed. Knowing the factor of weight per unit area for the paper and the magnification, the true area of contact could be determined. A planimeter was also used to measure the areas. The total area of contact is given in Table 8 for each specimen. Specimens G-4-P and G-5-P, which were tested at the higher sliding velocity, show considerably more area in contact than do the corresponding specimens (G-1-P and G-2-P) which were tested at the lower sliding velocity.

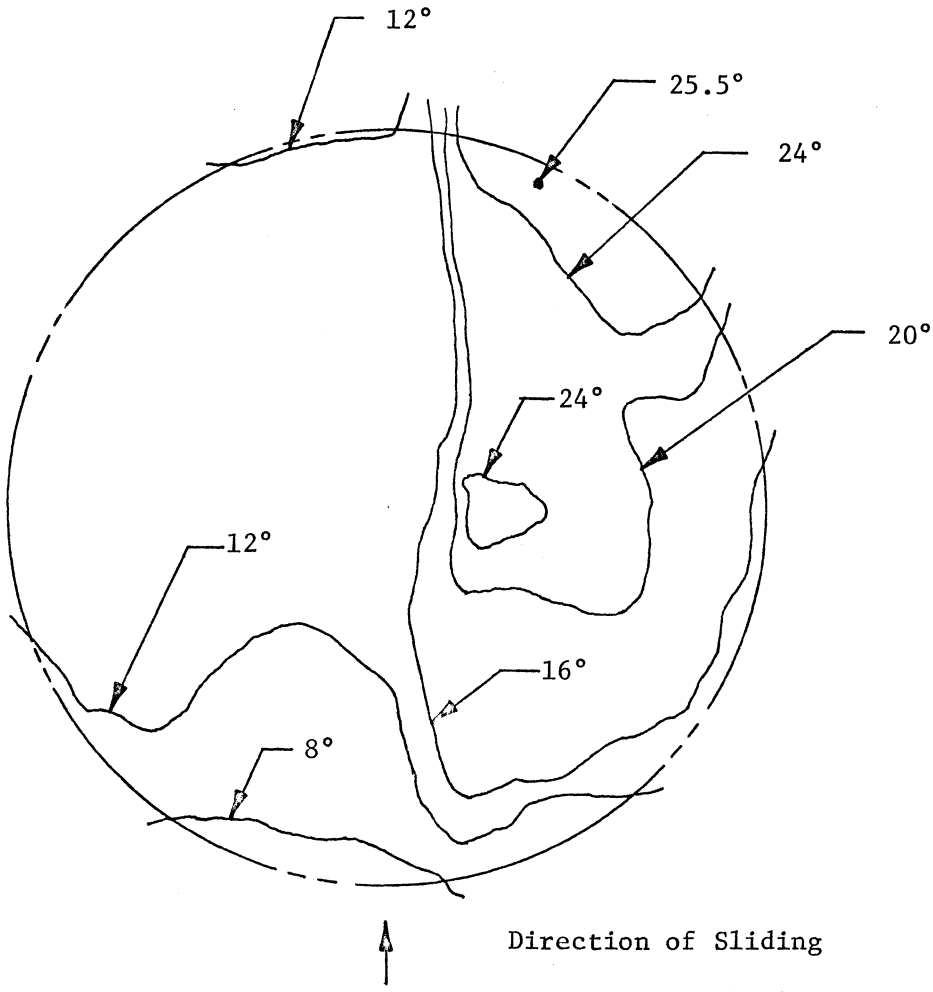

Figure 15

Temperature Rise Distribution (°K) Above Ambient for Specimen G-2-P

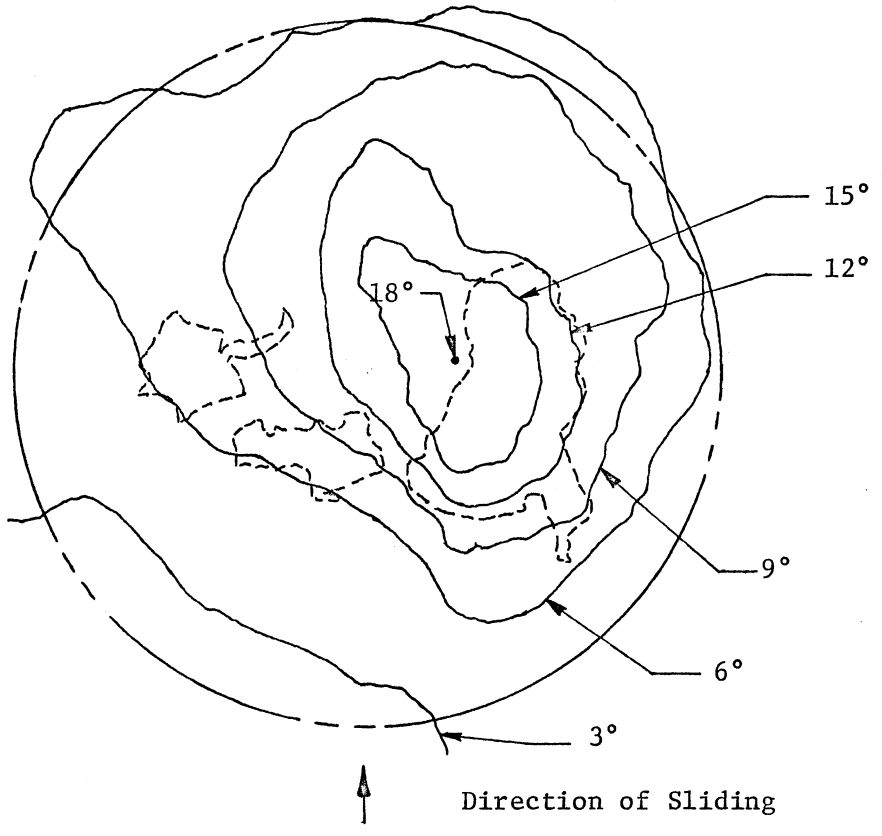

Figure 16

Temperature Rise Distribution (°K) Above Ambient for Specimen G-3-P

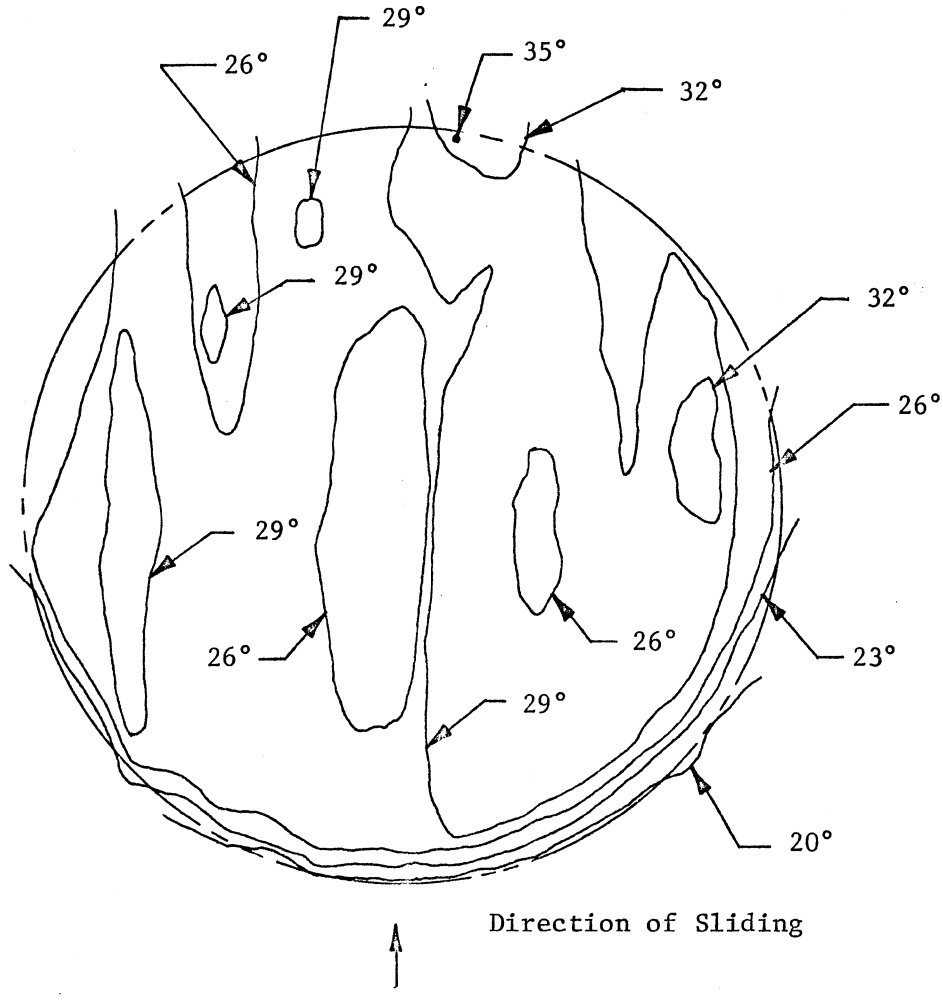

Figure 17

Temperature Rise Distribution (°K) Above Ambient for Specimen G-4-P

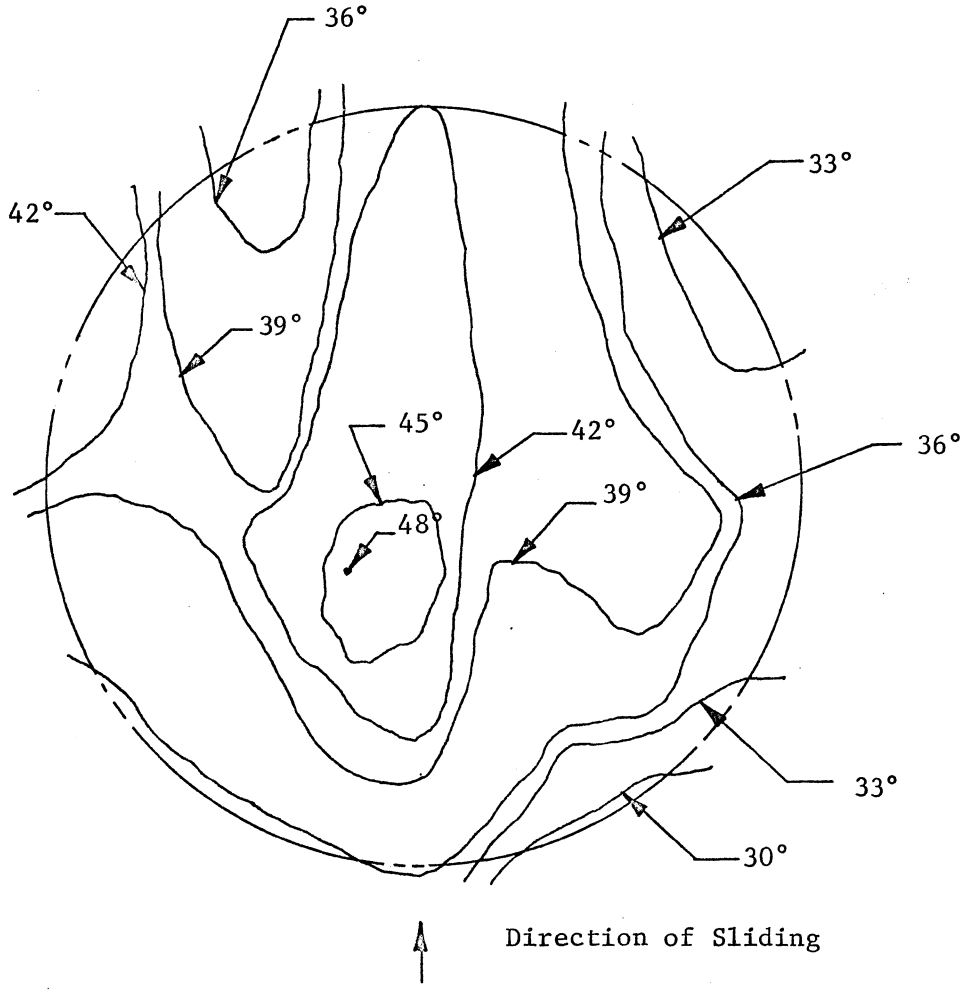

Figure 18

Temperature Rise Distribution (°K) Above Ambient for Specimen G-5-P

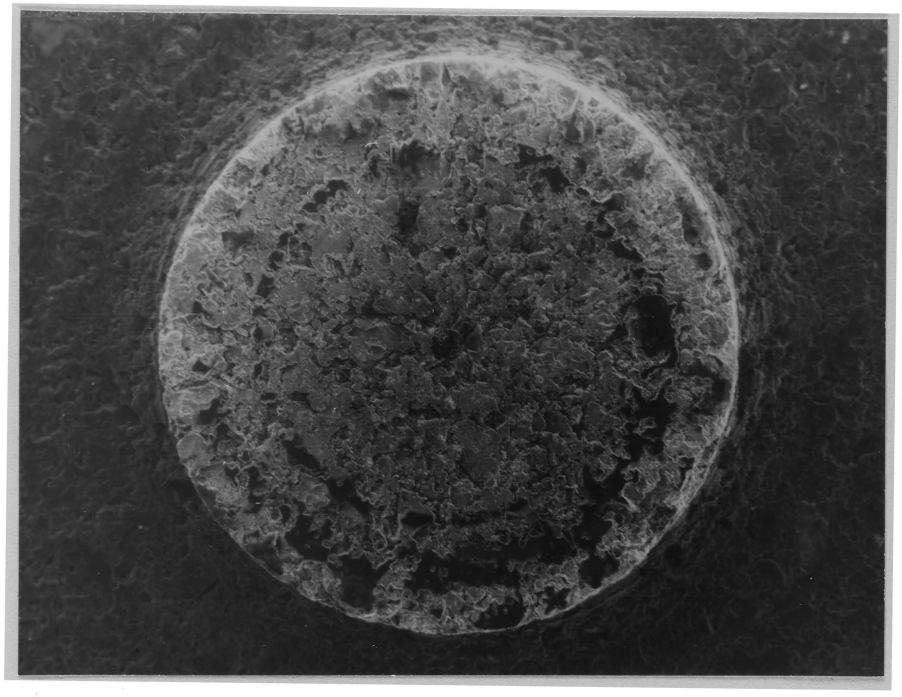

Direction of sliding

Figure 19

Surface of Specimen G-1-P After Testing (35X)

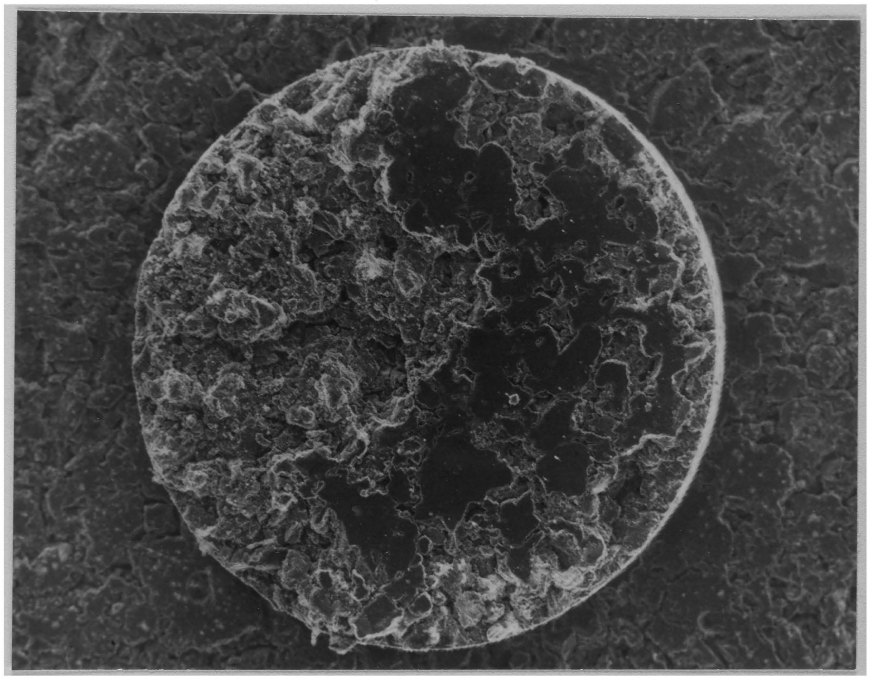

Direction of Sliding

Figure 20

Surface of Specimen G-2-P After Testing (70X)

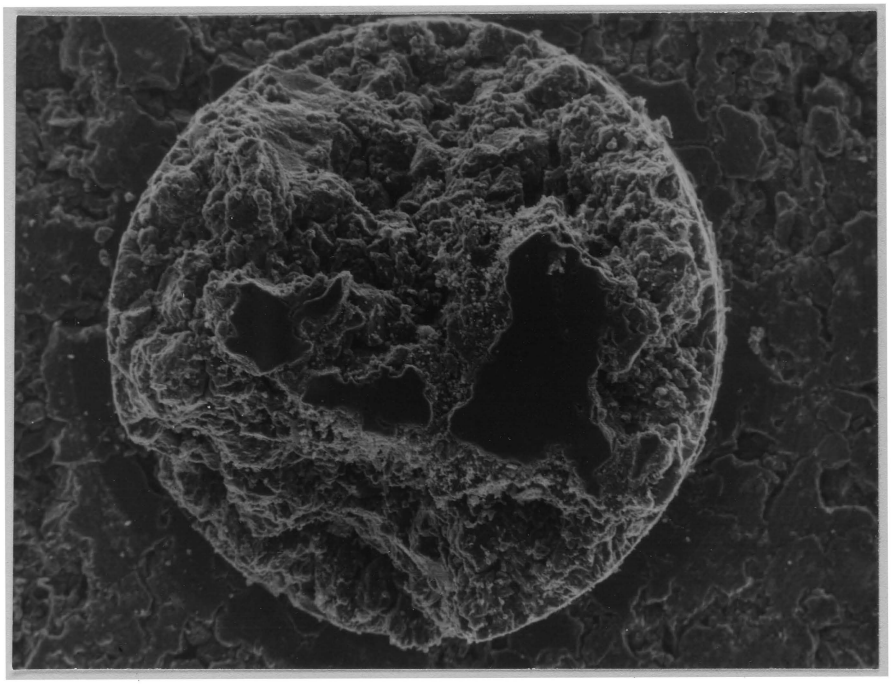

Direction of sliding

Figure 21

Surface of Specimen G-3-P After Testing (140X)

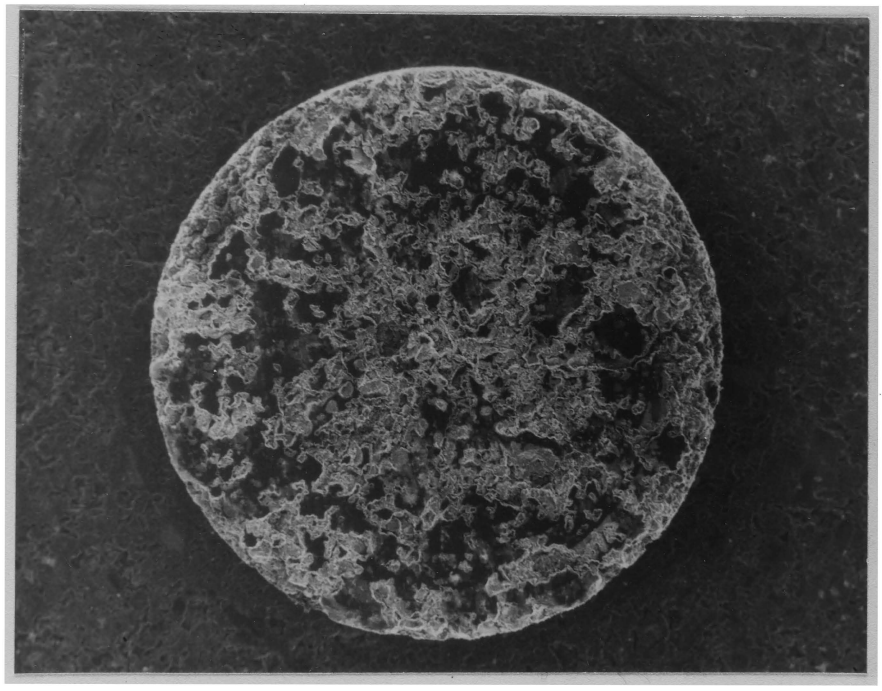

Direction of Sliding

Figure 22

Surface of Specimen G-4-P After Testing (35X)

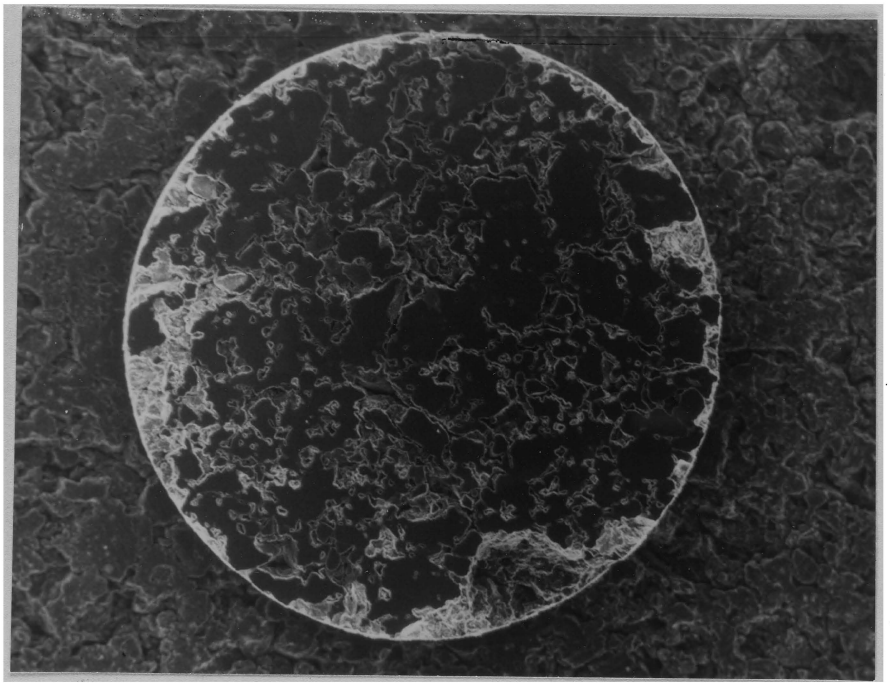

Direction of Sliding

Figure 23

Surface of Specimen G-5-P After Testing (70X)

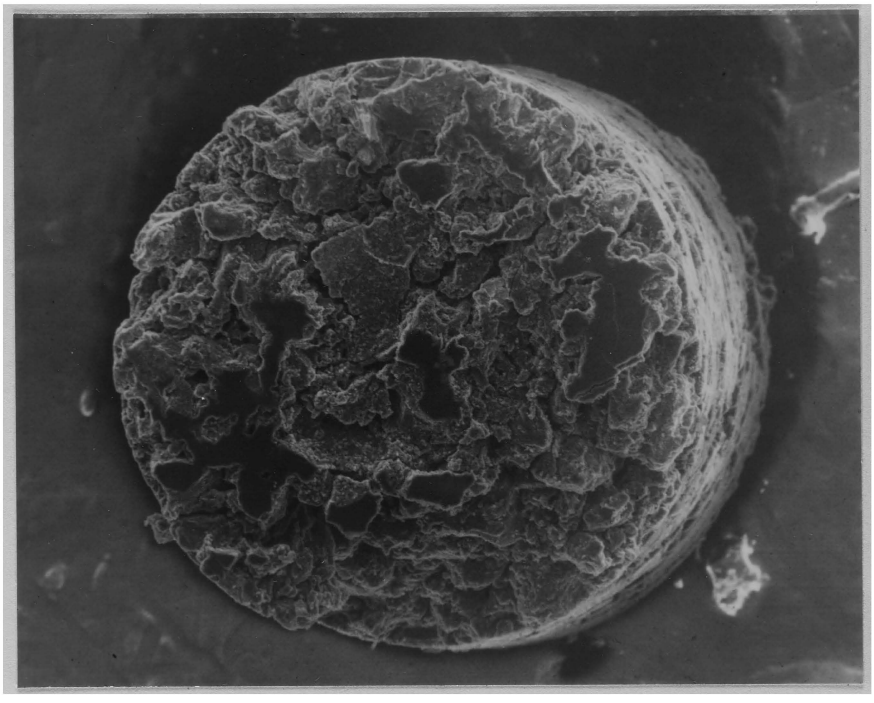

Direction of Sliding

Figure 24

Surface of Specimen G-6-P After Testing (140X)
(Tilted Approximately 4°)

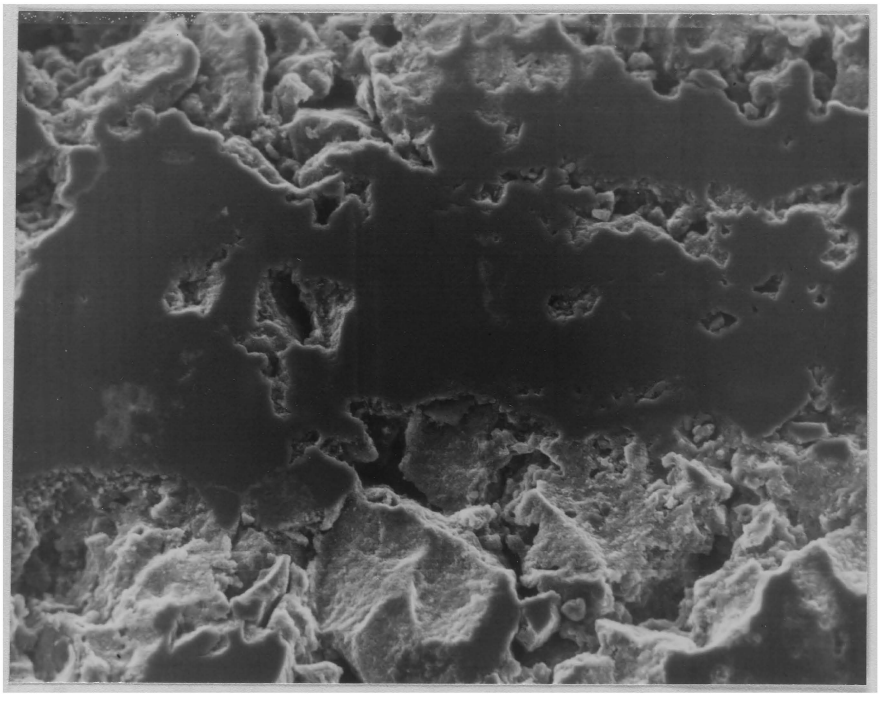

Direction of Sliding

Figure 25

Typical Wear Region on Graphite Specimen G-1-P (400X)

Table 8

True Area of Contact and Coefficient of Friction at Equilibrium

Specimen	True Area of Contact** (m^2)	Macroscopic Area of Contact (m^2)	Percent of Maximum Possible Area of Contact	Coefficient of Friction
G-1-P	4.48×10^{-7}	5.06×10^{-6}	9%	0.425
G-2-P	2.64×10^{-7}	1.27×10^{-6}	21%	0.564
G-3-P	2.89×10^{-8}	3.17×10^{-7}	9%	0.315
G-4-P	1.19×10^{-6}	5.06×10^{-6}	24%	0.678
G-5-P	6.71×10^{-7}	1.27×10^{-6}	53%	0.938
G-6-P*	2.52×10^{-8}	3.17×10^{-7}	8%	0.326

* Data at 3.6 minutes, not at equilibrium.

** Sum of areas of contact determined from scanning electron microscope photographs.

A typical trace of torque as a function of time is shown in Figure 26. The procedure for determining the coefficient of friction from this data is given in Appendix G. Although some fluctuation in the friction force was recorded throughout the tests, it was reasonably constant. The coefficient of friction at equilibrium for each test is given in Table 8.

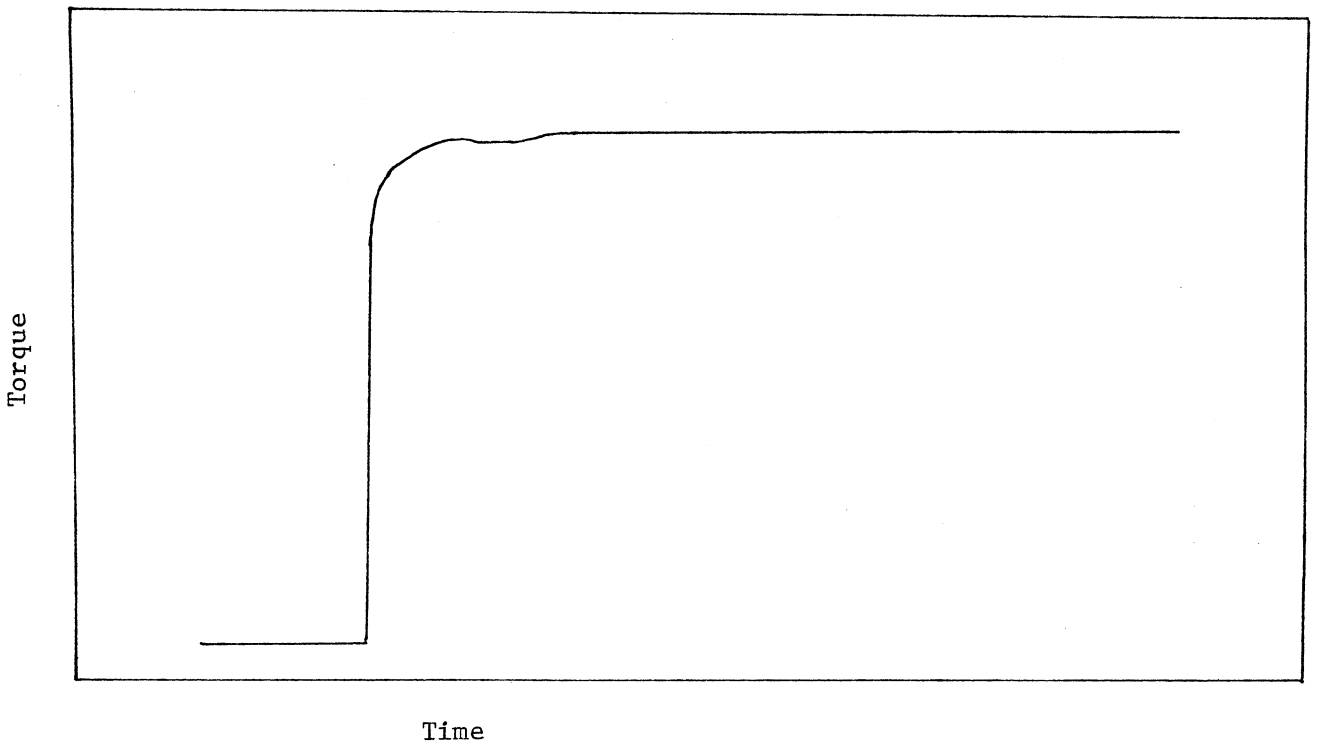

Figure 26

Typical Plot of Torque as a Function of Time

B. Theoretical

The theories of Blok, Holm, Archard, and Jaeger were used to make theoretical calculations of the temperature rise based on the total area of contact determined from the scanning electron microscope photographs. Other areas which could be used in theoretical calculations are: a) macroscopic area (i.e., the cross-sectional area of the protusion) b) area based on plastic deformation of the graphite c) area based on the shear strength of the graphite and d) each individual area shown in the scanning electron microscope photographs. A comparison of these areas is given in Table 9.

The area based on plastic deformation is calculated from

$$\text{Area} = W/p_m$$

where W is the normal load and p_m is the hardness of graphite. The area based on the shear strength is obtained from

$$\text{Area} = F/S$$

where F is the friction force and S is the shear strength of the graphite. Archard's theory was used to determine the temperature rise based on these different areas.

The maximum temperature rise in a circular area of contact can be calculated using Blok's theory. For example, the data from test G-5-P, using the area of contact determined from the scanning electron microscope photographs, satisfy the high speed criterion (i.e., $V > 5(4\kappa/a)$). Therefore, the maximum temperature rise is calculated using equation 2* and is 15.2°K.

---

*Equation numbers refer to the equations presented in the literature review section of this thesis.

Table 9

Comparison of Possible Areas of Contact

Test Specimen	Macroscopic Area (m^2)	Area from SEM (m^2)	Area Based on Plastic Deformation (m^2)	Area Based on Shear Strength (m^2)
G-1-P	5.06×10^{-6}	4.48×10^{-7}	7.69×10^{-9}	7.66×10^{-8}
G-2-P	1.27×10^{-6}	2.64×10^{-7}	7.69×10^{-9}	1.06×10^{-7}
G-3-P	3.17×10^{-7}	2.77×10^{-8}	7.69×10^{-9}	5.68×10^{-8}
G-4-P	5.06×10^{-6}	1.19×10^{-6}	7.69×10^{-9}	1.22×10^{-7}
G-5-P	1.27×10^{-6}	6.71×10^{-7}	7.69×10^{-9}	1.69×10^{-7}
G-6-P	3.17×10^{-7}	2.52×10^{-8}	7.69×10^{-9}	5.87×10^{-8}

Holm's theory also predicts the maximum temperature rise in the area of contact. Again, using data from test G-5-P and the area of contact from the scanning electron microscope photographs, the value of the dimensionless parameter B(z) may be obtained from Figure 3 of Blok's paper (17) and is 0.95. The maximum temperature rise is 94.°K as calculated from equation 11.

The mean temperature rise in the area of contact can be calculated using Jaeger's theory. Data from test G-5-P, using the area of contact determined from the scanning electron microscope photographs, satisfy the high speed criterion (i.e., $L > 5$) so that equation 4 can be used. The mean temperature rise in the area of contact is 9.7°K.

Archard's theory also predicts the mean temperature rise. If the same data is used as in the above examples, equations 9 and 10 can be used. The mean temperature rise using Archard's analysis is 12.4°K.

Table 10 gives a comparison of the temperature rise for each specimen using the four theories. The total contact area as determined from the scanning electron microscope photographs was used in these calculations. Figures 27 and 28 are plots of the theoretical temperature rise versus the experimental temperature rise.

Archard's theory was used to investigate the different mean temperature rises based on different contact areas. Four possible areas of contact were chosen. The largest possible area of contact is equal to the cross-sectional area of the protuberance on each

Table 10

Comparison of Experimental and Theoretical Temperature Rise (^{o}K)

Test Specimen	Experimental at Center	Experimental Maximum	Blok (maximum)	Holm (maximum)	Jaeger (mean)	Archard (mean)
G-1-P	5.5	-	4.0	13.5	2.7	3.8
G-2-P	12.4	25.5	7.7	13.2	5.8	6.0
G-3-P	13.4	18.5	18.9	39.6	13.7	13.6
G-4-P	24.0	35.5	7.3	51.0	4.6	5.8
G-5-P	43.6	48.5	15.2	94.0	9.7	12.4
G-6-P*	43.5	-	53.4	175.8	35.3	50.5

* Data at 3.6 minutes, not at equilibrium.

NOTE: All theoretical calculations in this table are based on a single circular area of contact equal to the total area of contact as determined from scanning electron micrographs.

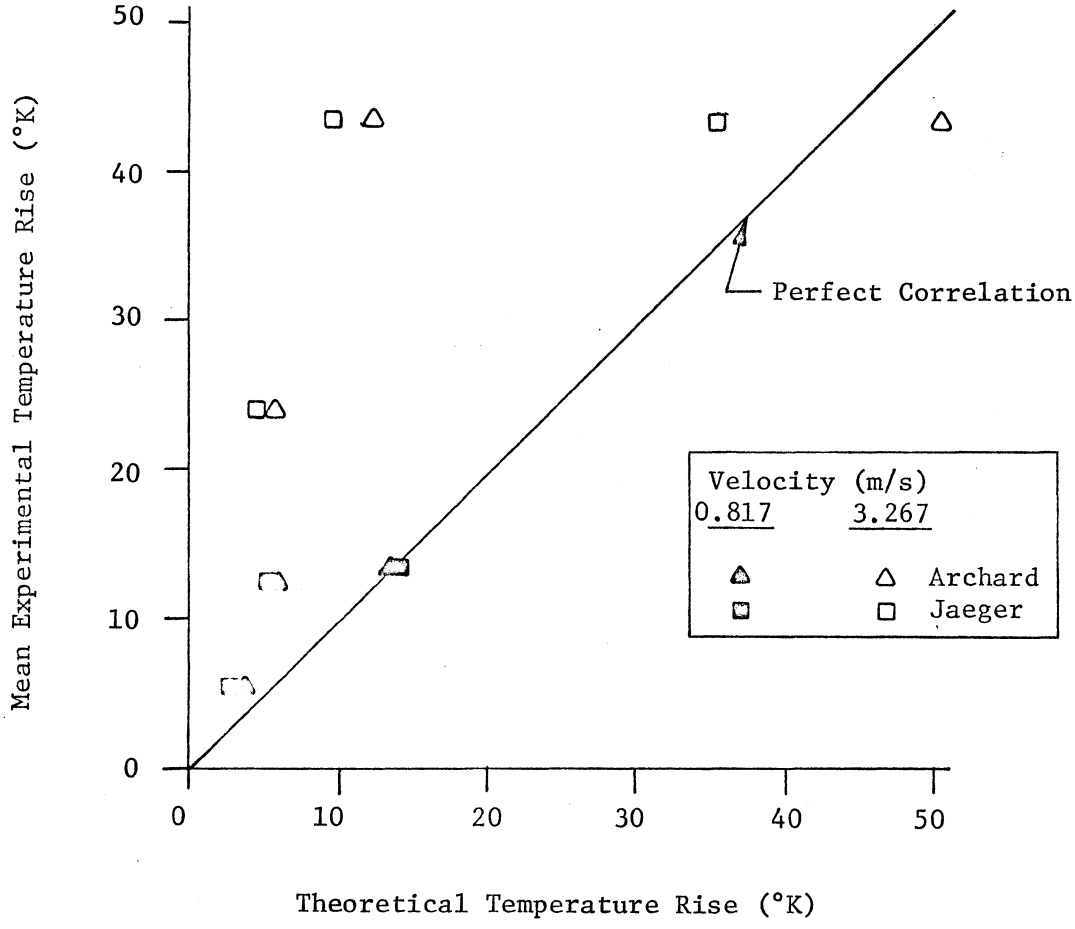

Figure 27

Mean Experimental Temperature Rise vs.

Theoretical Temperature Rise

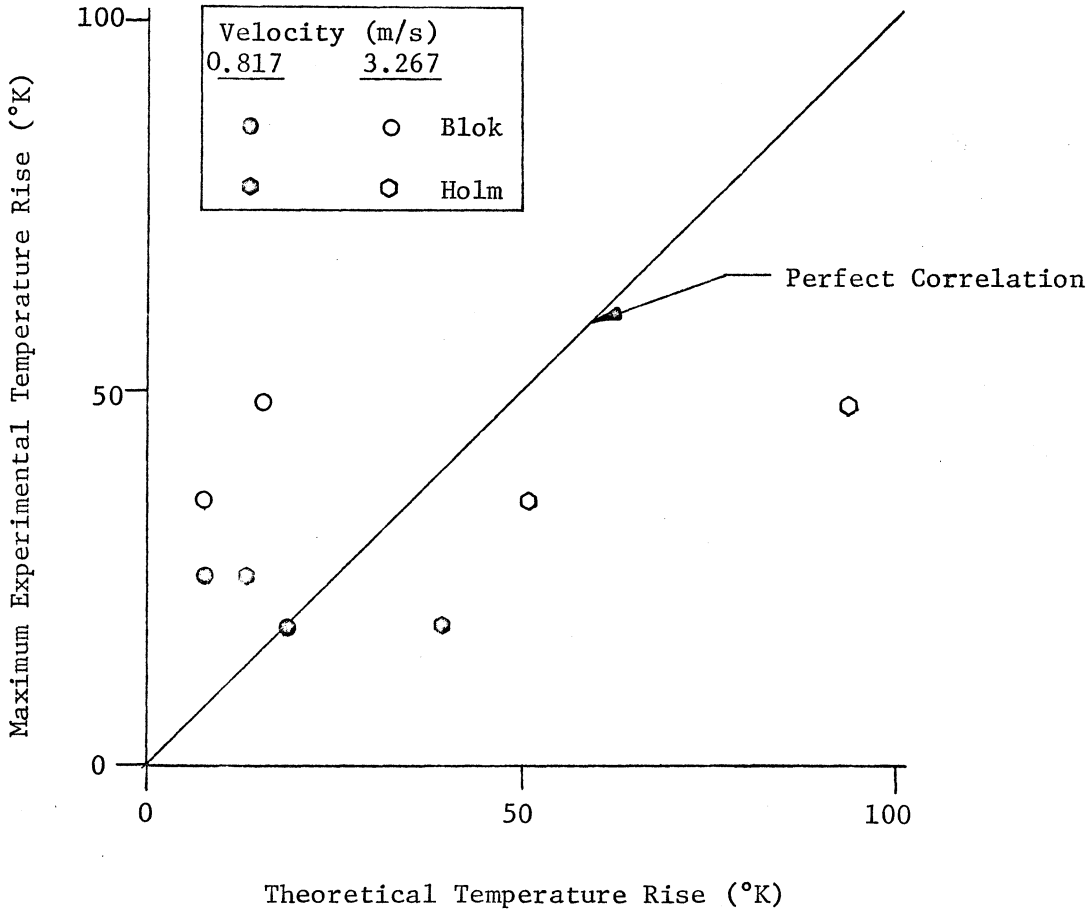

Figure 28

Maximum Experimental Temperature Rise

vs. Theoretical Temperature Rise

specimen. The area of contact determined from the scanning electron microscope photographs is the best approximation of the actual area of contact. The area of contact based on plastic deformation of the graphite and on the shear strength of graphite are two other areas which can be considered. Table 11 gives a comparison of the mean temperature rise based on these four areas.

All of the above analysis has been based on a single continuous area of contact. However, the scanning electron microscope photographs reveal that the area of contact is actually composed of many irregularly shaped smaller areas. A theoretical analysis which would calculate the temperature rise of each individual area could be performed. Specimen G-3-P was chosen for this analysis since it has only three areas of contact. Archard's analysis was used with the following assumptions; a) the load on each area was proportional to its percentage of the total area in contact, b) the coefficient of friction was the same for all areas, c) the sliding velocity was the same for all areas, and d) there was no interaction between the areas. The two smaller areas (refer to Figure 21) were of the same size (3.88×10^{-9} m^2) but of different shapes. The size of the larger area was 1.99×10^{-8} m^2. The results of the analysis are shown in Table 12. This analysis was not performed on the other specimens due to the large number of areas and their irregular shape.

Table 11

Comparison of Temperature Rise and the Area of Contact Using Archard's Theory

Specimen	Mean Temperature Rise (°K) for Macroscopic Area	for Area from SEM	for Area Based on Plastic Deformation	for Area Based on Shear Strength
G-1-P	0.6	3.8	42.2	9.9
G-2-P	2.3	6.0	56.0	10.7
G-3-P	3.7	13.6	31.3	8.9
G-4-P	2.0	5.8	187.0	32.2
G-5-P	7.7	12.4	258.7	34.9
G-6-P	7.6	50.5	89.9	26.8

Table 12

Temperature Rise of the Individual Areas of Specimen G-3-P Using Archard's Theory

Area (m^2)	Load (N)	Peclet Number	Mean Temperature Rise (°K)	
			Experimental	Theoretical
3.88×10^{-9}	0.27	0.57	7.6	6.7
3.88×10^{-9}	0.27	0.57	7.6	6.7
1.99×10^{-8}	1.42	1.30	14.2	12.4

DISCUSSION

A major objective of this investigation was to compare the temperature rise in the area of sliding contact as measured experimentally with that calculated from the theories of Blok, Archard, Jaeger, and Holm. The comparison between mean experimental temperature rise and the mean temperature rise calculated from the theories of Archard and Jaeger is shown in Figure 27. One can see that the agreement is reasonably good. For the low speed tests, specimen G-2-P (intermediate diameter) showed the largest difference between experiment and theory. But this difference was only 6.6°K. A larger difference between experiment and theory is evident for the tests conducted at the high velocity. The maximum difference of 33.9°K occurred for specimen G-5-P (intermediate diameter). Specimen G-6-P (smallest diameter) broke before reaching equilibrium so the comparison between theory and experiment was made with the data obtained at the time it broke. It is interesting to note that in nine out of twelve cases, the mean experimental temperature rise is greater than that predicted by theory. In two of these cases the theoretical prediction is no more than 0.3°K above the experimental value. The other case is for specimen G-6-P which broke before reaching equilibrium. This is much better agreement than obtained in studies with the dynamic thermocouple. For example with constantan alloy on steel, Furey (10) obtained mean experimental temperature rises which were approximately one-seventh the values predicted by Archard's theory. But in his study, the true area of contact was not known.

The comparison between the maximum temperature rise obtained from theory and experiment is shown in Figure 28. The maximum temperature rise as predicted by Blok's theory is lower than the experimental values in all cases but one. The largest difference was 33.3°K for specimen G-5-P (high velocity, intermediate diameter). However the temperature rise predicted by Holm's theory is greater than the experimental values in all cases but one. Specimen G-5-P again had the largest difference which was 45.5°K.

Possible reasons for discrepancies between experiment and theory follow.

A. Experimental Errors

The determination of the experimental temperature rise depends on the emissivity of the graphite; thus it was measured using the infrared microscope instead of using handbook values. Four sets of emissivity measurements were conducted. These included the emissivity of the graphite surface, the emissivity of a wear spot on the graphite surface, the emissivity of the graphite surface in contact with the sapphire disk, and the emissivity of a wear spot in contact with the sapphire disk. It was found that the emissivity was a function of both temperature and contact. The emissivity of a wear spot in contact with the disk was 0.33 at 25.5°C and increased to 0.58 at 48.3°C (refer to Figure 11). The emissivity of the wear spot not in contact with the sapphire was higher. It increased from 0.45 at 26.0°C to 0.63 at 55.0°C. Two sets of experimental calculations were made; one based on the average emissivity of a wear spot in contact with the sapphire and one

based on emissivity as a function of temperature of a wear spot in contact with the sapphire. For the low speed tests the difference was 1°K or less. For the high speed tests the difference ranged from 3.5°K to 7.5°K. However, the average emissivity value was used when making calculations to compare with theory because the basic comparison between experiment and theory was similar regardless of which emissivity was used.

Transfer of graphite to the sapphire disk was insignificant in all tests. It could not be detected visually. However when the sapphire disk was wetted with distilled water, the resulting pattern corresponded to the area of contact between the graphite and sapphire. If transfer did occur it could attenuate the infrared radiation from the area of contact which would lead to a lower experimental temperature rise. But the sliding system would then be graphite on graphite which theoretically would give a higher temperature rise. However the amount of transfer was insignificant in this study.

B. Theoretical Problems

Problems associated with the use of the theories fall into two main categories. The first is that the theories may be inadequate or have weaknesses. The second is that the theories are correct but the proper input is not being used.

One weakness of all the theories is that they do not include wear. Some of the energy supplied to the contact area (i.e., frictional energy) may be used to break away wear particles instead of

contributing to the temperature rise. Although no wear debris was observed in any of the tests, the scanning electron micrographs show a change in the surface of the graphite that was in contact with the sapphire.

None of the theories considers phase changes or chemical effects in the area of contact. One of the rubbing members may experience a phase change due to the increase in temperature; but in this study, this is not felt to be likely. Oxidation could conceivably occur with increased temperature. An exothermic reaction (e.g., $C + O_2 \rightarrow CO_2$) could take place at the interface thereby increasing the temperature.

All the theories model each member in a sliding system as an infinite heat sink. This may not always be an acceptable assumption. An embedded thermocouple was used to measure the bulk temperature rise of four of the graphite specimens. It was found to be insignificant in all but one of the specimens. Specimen G-5-P (high velocity, intermediate diameter) experienced a bulk temperature rise of 4.5°K but this was only approximately 10% of the mean temperature rise in the area of contact.

The basic theory may need refining in other ways. Although the theories of Archard and Jaeger give similar results, the theories of Blok and Holm give considerably different results. This indicates that more theoretical work needs to be done, particularly in the area of predicting the maximum temperature rise.

Not using or having the proper input for the theories would lead to differences between experimental and theoretical temperature rises.

The thermal and physical properties of a substance are usually a function of temperature. For example, the hardness of many materials is a function of temperature, decreasing as the temperature increases. At high sliding speeds the increase in temperature at the interface could cause the hardness to decrease. This would lead to a larger area of contact and a smaller increase in surface temperature. However SA-35 graphite has a very high melting point (approximately 3500°C) so the effect of temperature on hardness would be insignificant for the temperature rises measured in this study. All the properties of graphite and sapphire were considered constant.

The nature of the contact area (i.e., the size, shape and distribution of the areas of contact) is very important. All the theories assume the area of contact to be a single, continuous, geometrically simple area. The scanning electron micrographs show that the area of contact between graphite and the sapphire disk is composed of many small, irregularly shaped areas of contact. If the total area of contact is held constant and the number of areas in contact is allowed to increase, the calculated Archard temperature rise decreases markedly (see Appendix I).

The size of the area of contact is frequently calculated from plastic deformation (i.e., hardness). But the area of contact for graphite on sapphire as determined from the scanning electron micrographs is 3 to 150 times greater than that based on plastic deformation. A better approximation of the area of contact is obtained by basing it on the shear strength of graphite. Then the area of contact as

determined from the scanning electron microscope is 0.4 to 9.8 times the area based on the shear strength of the graphite.

Specimen G-3-P (smallest diameter, low velocity) was chosen for a detailed analysis of the individual areas of contact. Table 13 gives a comparison of experimental and theoretical temperature rises for the individual areas. Two values of experimental temperature rise are given. One value was calculated from the average emissivity (0.44); the other from an iteration procedure to determine an emissivity which corresponded to the approximate temperature rise. The temperature rise based on an average emissivity and the temperature rise based on emissivity as a function of temperature are within 1°K of each other except for one case in which there is a 3°K difference. For this specimen, the mean as well as maximum temperature rises predicted by the theories are within approximately 50% of the experimental values except for one case, the Holm prediction for area 3. Here the theoretical value is roughly twice the experimental maximum.

C. Summary

Overall the experimental data are felt to be accurate. The emissivity of the graphite was measured using the infrared microscope instead of using data from handbooks. The scanning electron microscope was used to determine the size and distribution of the areas of contact for each specimen. The agreement between experiment and theory was reasonably good. The detailed analysis of the individual areas of contact for specimen G-3-P (smallest diameter, low velocity) showed

TABLE 13

Experimental and Theoretical Temperature Comparisons

for Individual Areas of Contact for Specimen G-3-P

	Temperature Rise (°K)					
	Mean			Maximum		
Experimental	Area* 1	2	3	Area 1	2	3
Average emissivity	7.6	7.6	14.2	10.4	11.3	17.8
Emissivity as a function of temperature	8.4	8.4	14.2	11.3	14.3	17.4
Theoretical						
Archard	6.7	6.7	12.4			
Jaeger	10.5	10.5	15.8			
Blok				8.5	8.5	16.2
Holm				16.8	16.8	39.1

*

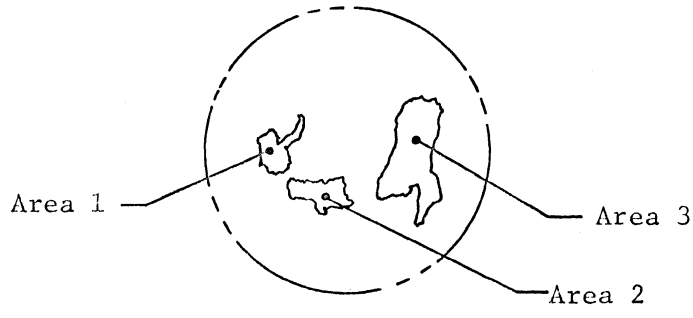

particularly good agreement between experiment and theory (i.e., within 50%).

CONCLUSIONS

An experimental apparatus was used to measure the temperature rise above ambient in the area of contact in a well-characterized sliding system. The sliding system consisted of a pure graphite (Union Carbide SA-35) spherical test specimen with a cylindrical protrusion which was loaded against a rotating, optically flat sapphire disk; the axis of the cylinder was normal to the plane of the disk. A Barnes Infrared Microscope was used to measure the radiance from the area of contact. The mean temperature rise and the temperature rise distribution over the area of contact could be determined from the radiance data coupled with emissivity measurements. The experimentally measured temperature rises were compared with the temperature rises as predicted by the theories of Blok, Archard, Jaeger, and Holm.

The conclusions from this investigation are as follows:

[1] The experimental apparatus was successfully adapted to obtain data on friction and radiance from the area of contact of pure, cylindrical graphite specimens sliding on a rotating sapphire disk. Data were obtained for two speeds (0.817 m/s and 3.267 m/s), one load (1.96 N), and three different specimen diameters (0.63×10^{-3}m, 1.27×10^{-3}m, and 2.54×10^{-3}m).

[2] The emissivity of the graphite test specimens was measured using the infrared microscope and found to be a function of temperature, contact and wear. The emissivity increased as the temperature increased. The emissivity was lower for

the graphite in contact with the sapphire than for the graphite alone. The emissivity values for a wear spot were lower than those for the "as machined" surface.

[3] The mean temperature rise increased as the size of the graphite test specimens decreased.

[4] The mean temperature rise in the area of contact for the tests conducted at the high velocity (3.267 m/s) was approximately four times greater than the mean temperature rise for the low velocity (0.817 m/s) tests.

[5] The temperature rise distribution over the macroscopic area of contact corresponds approximately to the areas of contact determined from the scanning electron micrographs.

[6] The bulk temperature rise of the graphite test specimens was insignificant for all tests.

[7] The total area of contact as determined from the scanning electron micrographs (SEM) was roughly two orders of magnitude greater than the calculated area of contact based on plastic deformation (i.e., hardness). Furthermore, the SEM areas averaged approximately four times greater than the calculated areas of contact based on the shear strength of the graphite (Bowden and Tabor adhesion theory).

[8] The boundary of the macroscopic area of contact could be easily determined from the radiance data.

[9] At the low velocity, the mean temperature rise predicted by the theories of Archard and Jaeger was within approximately 50% of the experimentally measured mean temperature rise.

[10] At the high velocity, the mean temperature rise predicted by the theories of Archard and Jaeger was approximately one-fourth the experimentally measured mean temperature rise.

[11] The maximum temperature rises predicted by the theories of Blok and Holm are considerably different. The experimental values of maximum temperature rise were approximately three times as large as those calculated using Blok's theory. But the experimental values were approximately one-half the maximum temperature rise predicted by Holm's theory.

[12] In a more detailed study of one specimen (G-3-P; smallest diameter, low velocity), it was found that the theoretical values of temperature rise (both mean and maximum) were within approximately 50% of the experimental values for each of the three individual areas of contact.

These results show the necessity of measuring the real areas of contact in any study of surface temperatures generated by friction. Furthermore, these areas can best be approximated from scanning electron micrographs of the contact zone; calculated areas of contact from plastic deformation, for example, may lead to very large errors in calculated temperature rises.

APPENDIX A

Calibration of the Barnes Infrared Microscope

A Barnes Model RM121-1 Radiometric Calibration Source was used to calibrate the microscope. The calibration source consisted of an infrared radiation source cavity and a wide range temperature controller. The cavity temperature can be regulated over the range of 60°C to 230°C (±1°C). A thermocouple was inserted in the cavity as an independent means of checking the temperature in the cavity.

The following procedure was used to calibrate the microscope. The microscope was first zeroed using the digital voltmeter. Next the microscope was focused on the aperture of the source cavity and then rotated away from the cavity so it would not be heated. The source cavity temperature controller was set to the desired temperature and allowed to stabilize (about 30 min.). The microscope was then rotated back over the cavity and the output was read from the digital voltmeter. The temperature could then be calculated. This temperature was compared with that obtained from the thermocouple and with the temperature shown on the temperature scale on the front of the microscope control unit. (Note: When using the 36X objective the focusing ring must be set to "0".)

Since the output of the microscope was in millivolts, it was necessary to know the radiance per volt factor. A radiometric scale with a range of 0 to 10 mw/ster - cm^2 was provided on the meter of the control unit. To obtain the radiance-per-volt factor, the milli-

volt output of the microscope was measured with the radiometric scale reading zero. Next the millivolt output of the microscope was measured with the radiometric scale at full deflection. The radiance per volt factor was then obtained by dividing the full scale radiance value by the change in voltage output of the microscope.

For example, the output of the microscope with the 36X objective and the radiometric scale reading zero was -2 millivolts. The output was 343 millivolts at full deflection of the radiometric scale. Therefore the radiance per volt factor was 10 mw/ster - cm^2 divided by 345 millivolts or .029 w/ster - cm^2 per volt.

Table A-1

Microscope Calibration

Source Setting (°C)	Microscope Reading: Digital Volt Meter (°C)	Microscope Reading: Temperature Scale (°C)	Thermocouple (°C)
66.0	64.0	65.0	68.0
72.5	71.0	71.0	71.0
107.0	105.0	105.0	104.4
132.5	136.0	131.0	130.0

Instrumentation

1. Barnes Infrared Radiometric Microscope

   Model RM-2A

   SN 412

2. Beck Reflecting Objective (36X)

   Model RM-163

   SN 255

3. Barnes Radiometric Calibration Source

   Model RM 121-1

   SN 307

4. Honeywell Digital Voltmeter

   Model 620B

   SN 3771093

5. Biddle-Gray Millivolt Potentiometer

   Model 604003

   SN 33840

APPENDIX B

Calibration of the Torque Transducer

A Lebow Miniature Rotary Torque Transducer was used to measure the torque on the shaft holding the rotating sapphire disk. The friction force and the coefficient of friction between the specimen and the sapphire disk could be determined with this apparatus.

To calibrate the torque transducer, the power input shaft (lower end) was clamped so no movement could occur. The sapphire disk was replaced by an aluminum disk 5.08×10^{-2} m in diameter and 6.4×10^{-3} m thick mounted on the upper shaft. A fine wire was wrapped around the edge of the disk and secured by a screw. A bowpan was attached to one end of the wire which was resting on a ball bearing support. Counterweights were attached to the other end of the wire (also on a ball bearing support). Thus no torque was applied to the shaft of the torque transducer. A Honeywell chart recorder was recording the output of the torque transducer. Weights were then added in increments to the bowpan until full deflection was obtained on the recorder. This procedure was repeated for different settings (1mv, 2mv, etc.) of full deflection on the recorder. A calibration curve of torque versus millivolt output of the torque transducer was made for each setting of full deflection on the Honeywell recorder.

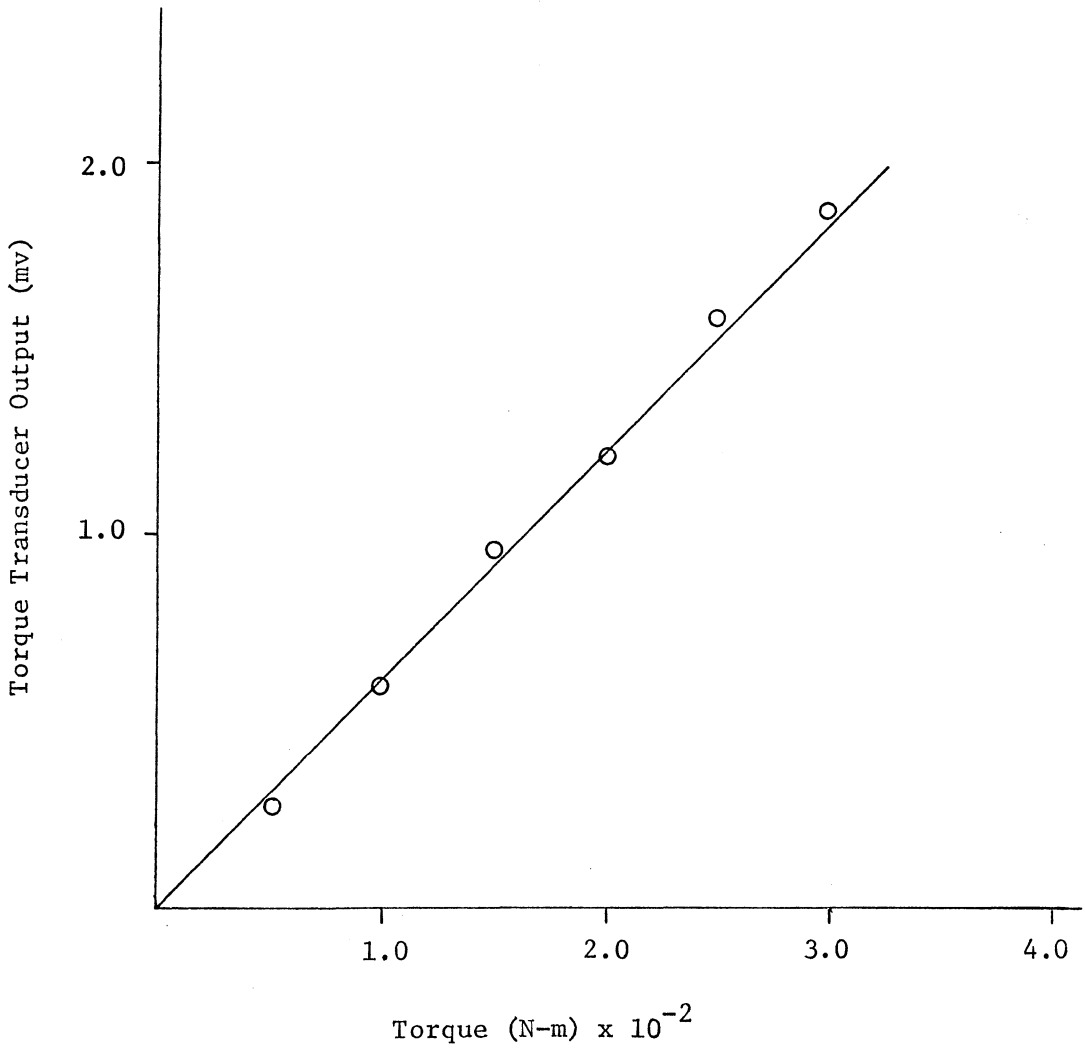

Figure B-1

Torque Transducer Calibration Curve

for 2.0 mv Full Deflection

Instrumentation

1. Lebow Miniature Rotary Torque Transducer

   Model 1102-50

   SN 752

2. Honeywell Brown Electronik Recorder

   Model No. Y153X17(VA)-X-30DN6

   SN 5421-N

3. Hewlett Packard DC Power Supply

   Model 721 A

   SN 412-20179

APPENDIX C

Calibration of the Linear Variable Differential Transformer

Linear variable differential transformers (LVDT) were attached to the precision X-Y table so the position of the microscope could be accurately determined. The output of one LVDT (either in the X or Y direction) was used as the X-axis input to the Moseley X-Y recorder to obtain a plot of radiance vs position.

Each LVDT was calibrated using the following procedure. The output of the LVDT was input to an Omega DC amplifier which in turn was connected to the X-axis of the Moseley recorder. The LVDT was adjusted to zero output with the aid of a digital voltmeter. The X-Y table was then moved a distance which corresponded to a displacement of one division along the X-axis on the Moseley recorder. The distance moved by the X-Y table was recorded. This procedure was repeated to cover the entire linear range of the LVDT ($\pm 2.54 \times 10^{-3}$ m) From this data a factor of displacement per division could be obtained.

Table C-1

LVDT Calibration Factors

X-axis Selector Setting (mv/DIV)	LVDT Calibration Factor $\times 10^5$ (m/DIV)	
	Radial	Tangential
10.0	1.575	2.108
20.0	3.175	4.242
50.0	7.874	10.922

NOTE: DIV = division = 2.54×10^{-2}m

Instrumentation

1. Linear Variable Differential Transformer

   Type 100HR - DC

   SN 1502 and 1503

2. Hewlett Packard Power Supply

   Model No. 6218A

   SN 1148A04942

3. Honeywell Digital Voltmeter

   Model 620 B

   SN 3771093

4. Omega DC Millivolt Amplifier

   Model Omni-Amp IIA

   SN DCMA - 3345

5. Moseley Autograph X-Y Recorder

   Model 2D

   SN 1217

APPENDIX D

Cleaning Procedures for the Sapphire Disk and the Graphite Specimens

The cleaning procedure for the sapphire disk was as follows;

1. The disk was scrubbed with a paper towel saturated with a detergent solution of tri-sodium phosphate (4% concentration).
2. A rinse with distilled water from a wash bottle followed.
3. The disk was immersed edge-wise in nitric acid (50% concentration) being careful not to let the epoxy or metal touch the acid.
4. Rinsed with distilled water.
5. The disk was immersed in 400 ml of hexane.
6. Rinsed with distilled water.
7. The disk was immersed in 400 ml acetone.
8. Rinsed with distilled water.
9. Methanol was poured over the disk to remove the water.
10. The disk was then stored in a desiccator until time for use.

The cleaning procedure for the graphite test specimens was as follows;

1. Each graphite specimen was heated by a bunsen burner to a dull red glow.
2. The heated specimen was then immersed in distilled water. This resulted in "explosive" removal of all the graphite dust particles due to machining.

3. The specimens were then placed in a vacuum oven at 60°C and 0.64 m Hg vacuum for two hours.

4. The specimens were stored in a covered glass container in a desiccator until time for use.

This procedure was recommended by Dr. P. M. Scherer of Union Carbide.

APPENDIX E

The Values of Θ_B, Θ_c, Θ_m and L Obtained from Archard's Analysis

The values of the mean temperature rise in the area of contact for the graphite, Θ_B, and for the sapphire disk, Θ_c, are calculated in Archard's analysis before obtaining the mean temperature rise, Θ_m, at the area of contact. Table E-1 lists these values for each test along with the Peclet number, L.

Table E-1

Θ_B, Θ_c, Θ_m and L Values Obtained from Archards Analysis*

Test	Mean Temperature Rise of Graphite, Θ_B (°K)	Mean Temperature Rise of Sapphire, Θ_c (°K)	Mean Temperature Rise in the Area of Contact (°K)	Peclet Number, L
G-1-P	10.8	5.9	3.8	6.2
G-2-P	18.6	8.7	6.0	4.7
G-3-P	31.5	24.1	13.7	1.6
G-4-P	42.2	6.8	5.8	40.2
G-5-P	77.7	14.6	12.4	30.2
G-6-P	139.4	79.3	50.5	5.85

* Based on singular, circular area of contact whose size is equal to the sum of the areas of contact as shown in the scanning electron microscope photographs.

APPENDIX F

Procedure for Measuring the Transmissivity of the Sapphire Disk

It was necessary to know the transmissivity (i.e., the fraction of incident energy that passes through a substance) of a sapphire disk since the microscope was viewing the area of contact through it. To obtain the transmissivity of the sapphire disk the following procedure was used.

The Barnes Radiometric Calibration Source was set to a given temperature and allowed to stabilize. The microscope was focused on the aperture of the cavity and the output was recorded. The sapphire disk was then inserted between the microscope objective and the cavity and the output recorded. This procedure was repeated for several different source temperatures. Care was taken so neither the microscope nor the disk was heated by the calibration source cavity.

Table F-1

Transmissivity of the Sapphire Disk

Calibration Source Temperature (°C)	Microscope Output (mv) Calibration Source	With Disk	Transmissivity
66.0	336	279	0.830
72.6	419	350	0.835
83.5	550	460	0.836
107.0	1020	850	0.833

average transmissivity -0.834

Instrumentation

1. Barnes Infrered Radiometric Microscope

   Model RM-2A

   SN 412

2. Beck Reflecting Objective (36X)

   Model RM-163

   SN 255

3. Barnes Radiometric Calibration Source

   Model RM121-1

   SN 307

4. Honeywell Digital Voltmeter

   Model 620 B

   SN 3771093

APPENDIX G

Procedure for Calculating the Coefficient of Friction

The output of the torque transducer was recorded on the Honeywell chart recorder. Calibration curves were made (see Appendix B) for different settings of full scale deflection on the recorder.

To obtain the coefficient of friction for a test, the percentage of full scale deflection was read from the Honeywell chart recording of that test at the desired elapsed time into the test. This percentage was multiplied by the full scale setting on the recorder to get the millivolt output of the torque transducer. The torque corresponding to this millivolt output was then read from the appropriate calibration curve. The coefficient of friction was then obtained by dividing this torque by the normal load and the radial distance of the specimen from the center of rotation of the sapphire disk.

Example Calculation

1. Test date: normal load: 1.96 N

   radial location of specimen: 1.733×10^{-2} m

2. At five minutes into the test the Honeywell recorder had a reading of 0.445 with a full scale setting of 2 millivolts.

Therefore the output of the torque transducer was (0.445) x (2.0) = 0.89 mv.

3. The torque corresponding to 0.89 millivolts was read from the 2.0 millivolt full deflection calibration curve. This torque was 1.44×10^{-2} N-m.

4. The coefficient of friction was then obtained by dividing the torque by the normal load and the radial distance.

$$\frac{1.44 \times 10^{-2}}{(1.96)\ (1.773 \times 10^{-2})} = 0.414$$

5. The coefficient of friction was 0.414 for this test.

APPENDIX H

Procedure for Calculating the Surface Temperature Rise of the Graphite Specimen

The output of the microscope was recorded by the Moseley X-Y recorder. This data, along with the transmissivity of the sapphire disk and the emissivity of the graphite, was used to calculate the surface temperature of the graphite.

The output from the microscope, at the desired elasped time, (as shown on the graph from the Moseley X-Y recorder) was multiplied by the radiance-per-volt factor of the microscope. This factor was obtained by taking the full scale radiance value of the microscope and dividing it by the corresponding voltage output of the microscope. The value of the product was then divided by the emissivity of the graphite and the transmissivity of the sapphire to obtain the radiance of the contact area. The radiance due to ambient temperature was added. This value of radiance was then used to determine the temperature of the area of contact by using the graph of radiance vs temperature supplied by Barnes Engineering Co. To obtain the temperature rise in the area of contact, the ambient temperature must be subtracted from the value read from the graph.

Example Calculation

1. The output of the microscope was 7.5 millivolts as read on the chart from the Moseley X-Y recorder.

2. This output was multipled by 0.029 (W/cm^2-ster)/volt which is the radiance per volt factor for the X1 setting on the microscope.

$$(7.5 \times 10^{-3})\ (.029) = 0.2175 \times 10^{-3}\ W/cm^2\ ster$$

3. Next the radiance value was divided by the emissivity of the graphite (0.441) and the transmissivity of the sapphire (0.83).

$$\frac{0.2175 \times 10^{-3}}{(0.441)\ (0.83)} = 0.594 \times 10^{-3} W/cm^2 - ster$$

4. The radiance due to ambient temperature of 20.5°C (3.0×10^{-3} W/cm^2 - ster) was added.

$$(3.0 + 0.594) \times 10^{-3} = 3.594 \times 10^{-3} W/cm^2 - ster$$

5. The temperature from the graph corresponding to this radiance was 26°C.

6. The ambient temperature (20.5°C) was subtracted to give the temperature rise of the contact area.

$$26 - 20.5 = 5.5°C$$

7. Therefore the temperature rise in the contact area was 5.5°C.

APPENDIX I

Effect of Subdividing the Area of Contact on the Temperature Rise

A computer program was written to aid in the study of the effect of subdividing the area of contact on the temperature rise using Archard's theory. The area of contact was assumed to be circular and based on plastic deformation of the graphite. This area was then divided into a number of smaller, equal-sized circular areas. The normal load was divided equally among the smaller areas. The load and speeds used in the experimental investigation were used for this study.

Figures I-1 and I-2 show that as the number of areas increased the temperature rise decreased. The decrease in temperature rise was rapid for smaller number of areas but as the number of areas increased the effect was much less. The step in Figure I-1 was due to a change from the intermediate equation to the low speed equation.

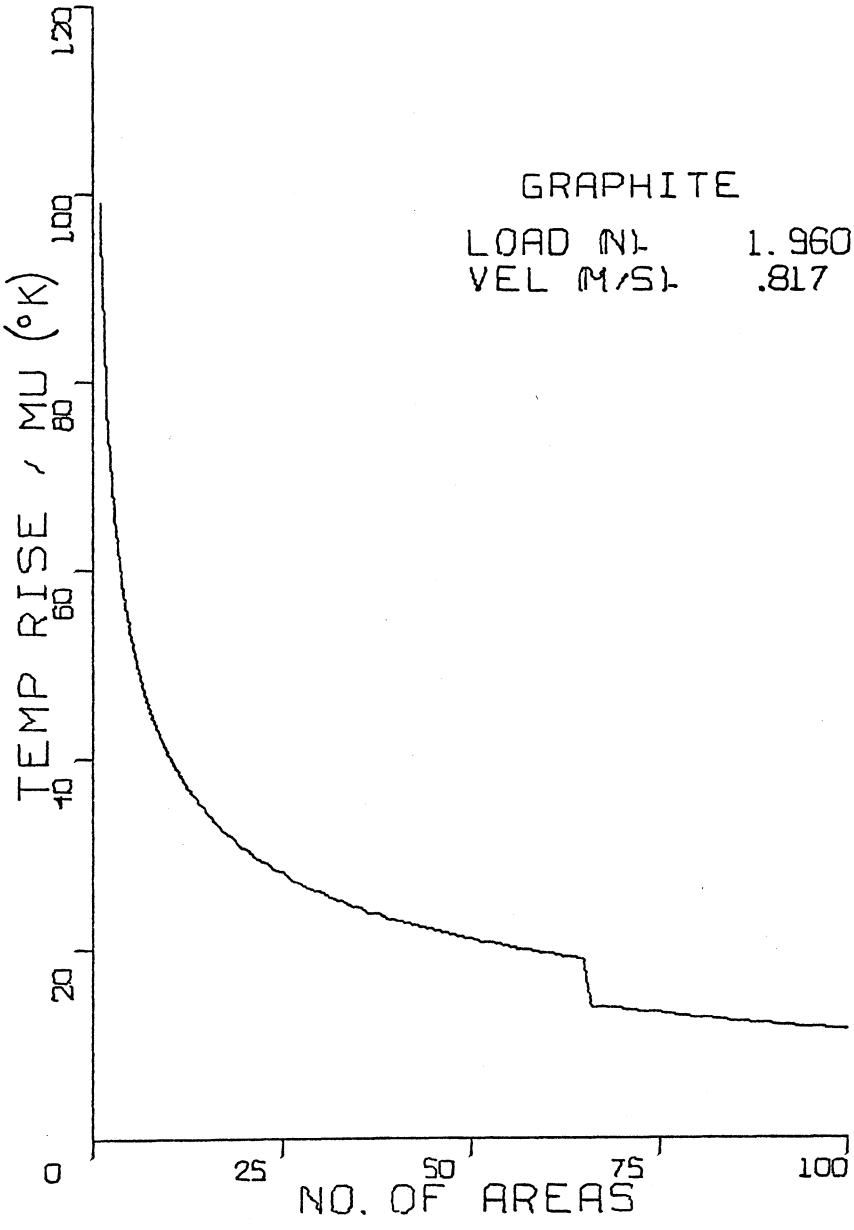

FIGURE I-1

EFFECT OF NUMBER OF AREAS ON TEMP RISE USING ARCHARD THEORY

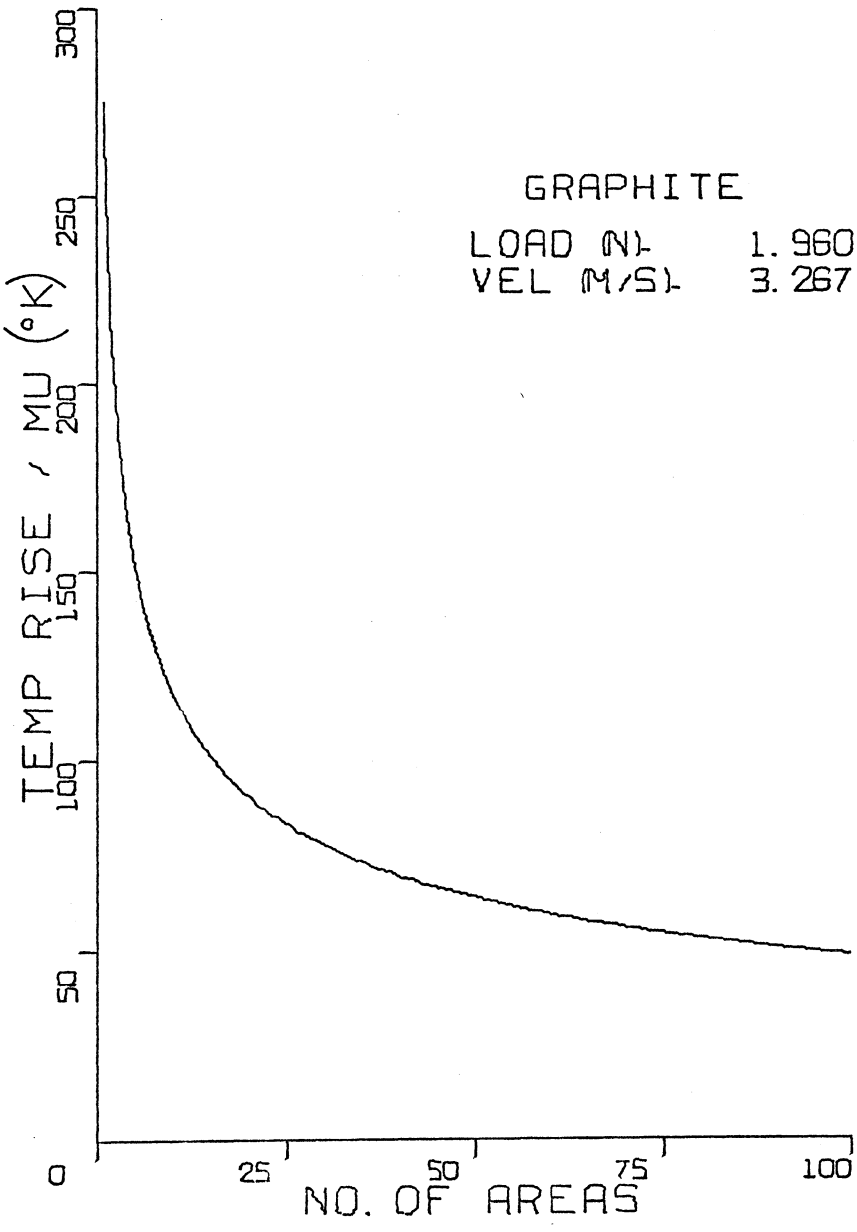

FIGURE I-2

EFFECT OF NUMBER OF AREAS ON TEMP RISE USING ARCHARD THEORY

```
      REAL KB,KC,MU,LE,LP,N
      DIMENSION ANN(101),TPU(100),THBU(100),THCU(100)
      DIMENSION TMPU(100),AN(101),LABELX(3),LABELY(4)
      DIMENSION BNAME(3), CNAME(3),CINV(100)
      READ(5,10) (BNAME(I),I=1,3),EB,RHOB,CB,KB,PMB,TMB,POISB
      READ(5,10) (CNAME(I),I=1,3),EC,RHOC,CC,KC,PMC,TMC,POISC
   10 FORMAT(2A4,A2,7F10.0)
      WRITE(6,170)
  170 FORMAT(1H1,'CALCULATION OF SURFACE TEMPERATURES'//)
      WRITE(6,190)
      WRITE(6,440)
  440 FORMAT(1H+,30X,'__________',5X,'__________'/)
  190 FORMAT(1H ,28X,'    SPHERE',5X,'     PLANE')
      WRITE(6,180) (BNAME(I),I=1,3),(CNAME(I),I=1,3),EB,EC,
     2RHOB,RHOC,CB,CC,KB,KC,PMB,PMC,TMB,TMC,POISB,POISC
  180 FORMAT(1X,'MATERIAL                              ',2A4,A2,5X,
     12A4,A2/1X,
     2          'MODULUS OF ELASTICITY(N/M**2) ',1PE10.4,5X,
     11PE10.4/1X,
     3          'DENSITY(KG/M**3)              ',1PE10.4,5X,
     11PE10.4/1X,
     4          'SPECIFIC HEAT(JOULES/KG-C)    ',1PE10.4,5X,
     11PE10.4/1X,
     5          'CONDUCTIVITY(JOULES/SEC-M-C)  ',1PE10.4,5X,
     11PE10.4/1X,
     5          'HARDNESS(N/M**2)              ',1PE10.4,5X,
     11PE10.4/1X,
     6          'MELTING POINT(C)              ',1PE10.4,5X,
     11PE10.4/1X,
     7          'POISSONS RATIO                ',1PE10.4,5X,
     11PE10.4/)
      READ(5,175) LABELX,LABELY
```

```
175  FORMAT(3A4,4A4)
     READ(5,31) K
31   FORMAT(I2)
     CALL PLOT(2.6,3.7,-3)
     DO 223 L=1,K
111  READ(5,30) W,V
30   FORMAT(2F10.3)
     WRITE(6,601) W,V
601  FORMAT(////,5X,'LOAD=',F10.4,'N',10X,'SPEED=',F10.4,
    1'M/S')
     AREA=W/PMB
     WRITE(6,602) AREA
602  FORMAT(/,5X,'AREA=',E10.4)
     WRITE(6,603)
603  FORMAT(//,5X,'NO. OF DIVISIONS',5X,'AREA OF EACH',5X,
    1'RADIUS',' OF EACH',7X,'PECLET NO.',5X,'THETA B /MU',
    25X,'THETA C /MU',5X,'TEMP RISE /MU')
     WRITE(6,610)
610  FORMAT(27X,'DIVISION',11X,'DIVISION')
     WRITE(6,612)
612  FORMAT(28X,'(M**2)',15X,'(M)',/)
     DO 1000 I=1,100
     AN(1)=1.
     AN(I+1)=AN(I)+1.
     N=KC/(RHOC*CC)
     AREAN=AREA/AN(I)
     AP=(AREAN/3.14175)**.5
     LP=V*AP/(2.*N)
     IF(LP.LE..1) TMPU(I)=(1./(KB+KC))*W*V/(4.*AP*AN(I))
     IF(LP.GT.5.) TMPU(I)=.31*W*V*SQRT(N/(V*AP))/(KC*AP*AN(
    1I))
     IF(LP.GT..1.AND.LP.LE.5.) TMPU(I)=((1.81*LP**(5./8.))
```

```
     1*W*V*N)/((4.*KB*(1.81*LP**(5./8.))*N*AP)+
     2(4.93*AP**2.*KC*V))/AN(I)
      THBU(I)=W*V/(4.*AP*KC)
      CINV(I)=(1./TMPU(I))-1./THBU(I)
      THCU(I)=1./CINV(I)
      WRITE(6,604) AN(I),AREAN,AP,LP,THBU(I),THCU(I),TMPU(I)
604   FORMAT(12X,F4.0,11X,E10.4,07X,E10.4,10X,E10.4,5X,F10.3,
     15X,F10.3,7X,F8.3)
1000  CONTINUE
      IF(TMPU(1).LE.90.) TIC=15.
      IF(TMPU(1).GT.90..AND.TMPU(1).LE.120.) TIC=20.
      IF(TMPU(1).GT.120..AND.TMPU(1).LE.270.) TIC=45.
      IF(TMPU(1).GT.270..AND.TMPU(1).LE.300.) TIC=50.
      IF(TMPU(1).GT.300.) TIC=100.
      DO 444 I=1,100
      TPU(I)=TMPU(I)/TIC
      ANN(I)=AN(I)*4./100.
444   CONTINUE
      CALL SAXIS(0.,0.,LABELX,-12,4.,0.,0.,25.,1.,0.)
      CALL SAXIS(0.,0.,LABELY,16,6.,90.,TIC,TIC,1.,1.)
      CALL SYMBOL(2.3,5.,.13,BNAME,0.,10)
      CALL SYMBOL(2.,4.7,.13,'LOAD (N)-',0.,10)
      CALL NUMBER(3.5,4.7,.13,W,0.,3)
      CALL SYMBOL(2.,4.5,.13,'VEL (M/S)-',0.,11)
      CALL NUMBER(3.5,4.5,.13,V,0.,3)
      CALL SYMBOL(1.1,-1.1,.13,'FIGURE I',0.,8)
      CALL SYMBOL(.1,-1.4,.13,'EFFECT OF NUMBER OF AREAS ON'
     1,0.,28)
      CALL SYMBOL(.1,-1.7,.13,'TEMP RISE USING ARCHARD
     1 THEORY',0.,37)
      J=1
      CALL PLOT(ANN(J),TPU(J),3)
```

```
      DO 333 I=1,100
      CALL PLOT(ANN(I),TPU(I),2)
333   CONTINUE
      CALL PLOT(0.,0.,3)
      CALL PLOT(10.,0.,-3)
223   CONTINUE
      CALL PLOT(0.,0.,-4)
      STOP
      END
```

REFERENCES

1. The Notebooks of Leonardo da Vinci, English translation by Edward MacCurdy, 1938, 2 Volumes.

2. Furey, M. J., "The Formation of Polymeric Films Directly on Rubbing Surfaces to Reduce Wear", Wear, Vol. 26, 1973, pp 369-392.

3. Wiggins, J. M., "An Experimental Method for Measuring Surface Temperatures Generated by Friction", Thesis, Virginia Polytechnic Institute and State University, Blacksburg, Virginia, 1975.

4. Omori, D. I., "Infrared Measurements of Surface Temperatures in an Unlubricated Sliding System", Thesis, Virginia Polytechnic Institute and State University, Blacksburg, Virginia, 1975.

5. Ling, F. F., and Simkins, T. E., "Measurement of Pointwise Juncture Condition of Temperature at the Interface of Two Bodies in Sliding Contact", ASME, Pittsburgh, 1962, Paper No. 62-Lub-14.

6. Quinn, T. J. F., "An Experimental Study of the Thermal Aspects of Sliding Contacts and Their Relation to the Unlubricated Wear of Steel", Proceedings of the Institution of Mechanical Engineers, Vol. 183, Pt. 3P, 1969, pp 129-137.

7. Santine, I. J., and Kennedy, F. E., "An Experimental Investigation of Surface Temperatures and Wear in Disk Brakes", ASLE/ASME Lubrication Conference, Montreal, 1974.

8. Vasilakis, J. D., "Apparatus for Surface Temperature Studies in Vacuum", The Review of Scientific Instruments, Vol 41, No. 4, April 1970, pp 521-527.

9. Bowden, F. P., and Ridler, K. E. W., "Physical Properties of Surfaces, III - The Surface Temperature of Sliding Metals, The Temperature of Lubricated Surfaces", Proceedings of the Royal Society, Vol. A154, 1936, pp 640-656.

10. Furey, M. J., "Surface Temperatures in Sliding Contact", ASLE Transactions, Vol. 7, 1964, pp. 133-146.

11. Cook, N. H., and Bhushan, B. "Sliding Surface Interface Temperatures", Journal of Lubrication Technology, Vol. 95, Jan. 1973, pp. 59-64.

12. Bowden, F. P., and Thomas, P. H., "The Surface Temperature of Sliding Solids", Proceedings of the Royal Society, Vol. 223, 1954, pp. 29-40.

13. Deyber, P., and Godet, M., "Contact Temperatures in Mixed Friction", Tribology, Vol. 4, August 1971, pp 150-154.

14. Winer, W. O., Sanborn, D. M., and Turchina, V., "Temperature Measurements in Sliding Elastohydrodynamic Point Contacts", ASME, New York, 1973, Paper No. 73-Lub-23.

15. Bowden, F. P., Stone, M. A., and Tudor, G. K., "Hot Spots on Rubbing Surfaces and the Detonation of Explosives by Friction", Proceedings of the Royal Society, Vol. 188, 1946, pp 329-349.

16. Kannel, J. W., and Dow, T. A., "The Evolution of Surface Pressure and Temperature Measurement Techniques for Use in the Study of Lubrication in Metal Rolling", Journal of Lubrication Technology, Vol. 96, October, 1974, pp 611-616.

17. Blok, H., "Theoretical Study of Temperature Rise at Surfaces of Actual Contact Under Oiliness Lubricating Conditions," General Discussion on Lubrication, London, 1937, Vol 2, Institution Mechanical Engineers, pp 222-235.

18. Archard, J. F., "The Temperature of Rubbing Surfaces", Wear, Vol. 2, 1958, pp. 438-455.

19. Holm, R., "Temperature Development in a Heated Contact With Applications to Sliding Contacts", Journal of Applied Mechanics, Vol. 19, September, 1952, pp. 369-374.

20. Jaeger, J. C., "Moving Sources of Heat and the Temperature at Sliding Contacts", Proceedings of the Royal Society N.S.W., Vol. 56, 1942, pp. 203-224.

21. Barnes Engineering Co. "Instruction Manual Infrared Radiometric Microscope Model RM-2A", 30 Commerce Road, Stamford, Conn.

22. Furey, M. J., "Friction, Wear and Lubrication", Industrial and Engineering Chemistry, Vol. 61, 1969, pp 12-29.

23. Furey, M. J., "The 'In Situ' Formation of Polymeric Films on Rubbing Surfaces", Colloques Internationaux du C.N.R.S., No. 233- Polymeres et Lubrification (Brest), publ. Paris, 1975, pp 393-404.

The vita has been removed from the scanned document

AN EXPERIMENTAL INVESTIGATION OF THE SURFACE TEMPERATURE OF GRAPHITE IN A SLIDING SYSTEM USING AN INFRARED MICROSCOPE

by

Melvin H. Richardson

(ABSTRACT)

Several very important problems remain unsolved in the field of Tribology. For example, we do not know the detailed nature and distribution of the real areas of contact when one solid body slides over another. Furthermore, we know very little about the actual surface temperatures produced in such systems. These two important unknowns are related and formed the basis for an investigation conducted at Virginia Polytechnic Institute and State University.

An experimental apparatus, using a sliding system, was constructed to study these problems. The sliding system consisted of SA-35 graphite test specimens loaded against a rotating sapphire disk. A scanning electron microscope was used to obtain detailed information on the size and shape of the areas of contact between the graphite and the sapphire. The surface temperature in the area of contact was determined by using a Barnes Infrared Microscope which measured the radiance from the area of contact. Since the target spot of the microscope was much smaller than the areas of contact, the temperature distribution over the macroscopic area of contact could be determined. The results of the experimental study were compared with the temperature rises in the area of contact predicted by the theories of Blok, Archard, Jaeger, and Holm. Possible reasons for discrepancies between theory and experiment were also examined.